The receptor MIK2 interacts with the kinase RKS1 to control quantitative disease resistance to Xanthomonas campestris

Florent Delplace, Carine Huard-Chauveau, Fabrice Roux, Dominique Roby

Plant Physiology®

Plant Physiology, 2025, **197**, kiae626
https://doi.org/10.1093/plphys/kiae626
Advance access publication 23 November 2024
Research Article

The receptor MIK2 interacts with the kinase RKS1 to control quantitative disease resistance to *Xanthomonas campestris*

Florent Delplace,* Carine Huard-Chauveau, Fabrice Roux, Dominique Roby*

Laboratoire des Interactions Plantes-Microbes Environnement (LIPME), INRAE, CNRS, Université de Toulouse, 31326 Castanet-Tolosan, France
*Author for correspondence: florent.delplace@inrae.fr (F.D.), dominique.roby.descazal@gmail.com (D.R.)
The author responsible for distribution of materials integral to the findings presented in this article in accordance with the policy described in the Instructions for Authors (https://academic.oup.com/plphys/pages/General-Instructions) is Carine Huard-Chauveau.

Abstract

Molecular mechanisms underlying qualitative resistance have been intensively studied. In contrast, although quantitative disease resistance (QDR) is a common, durable, and broad-spectrum form of immune responses in plants, only a few related functional analyses have been reported. The atypical kinase Resistance related kinase 1 (RKS1) is a major regulator of QDR to the bacterial pathogen *Xanthomonas campestris* (*Xcc*) and is positioned in a robust protein–protein decentralized network in Arabidopsis (*Arabidopsis thaliana*). Among the putative interactors of RKS1 found by yeast two-hybrid screening, we identified the receptor-like kinase MDIS1-interacting receptor-like kinase 2 (MIK2). Here, using multiple complementary strategies including protein–protein interaction tests, mutant analysis, and network reconstruction, we report that *MIK2* is a component of *RKS1*-mediated QDR to *Xcc*. First, by co-localization experiments, co-immunoprecipitation (Co-IP), and bimolecular fluorescence complementation, we validated the physical interaction between RKS1 and MIK2 at the plasma membrane. Using *mik2* mutants, we showed that *MIK2* is required for QDR and contributes to resistance to the same level as *RKS1*. Interestingly, a catalytic mutant of MIK2 interacted with RKS1 but was unable to fully complement the *mik2-1* mutant phenotype in response to *Xcc*. Finally, we investigated the potential role of the MIK2–RKS1 complex as a scaffolding component for the coordination of perception events by constructing a RKS1–MIK2 centered protein–protein interaction network. Eight mutants corresponding to seven RKs in this network showed a strong alteration in QDR to *Xcc*. Our findings provide insights into the molecular mechanisms underlying the perception events involved in QDR to *Xcc*.

Introduction

In response to pathogens, plants have developed complex resistance mechanisms that are either constitutively expressed or induced after a pathogen attack (Glazebrook 2005; Panstruga et al. 2009). Quantitative disease resistance (QDR) is the predominant form of resistance in crops and natural populations. QDR is characterized by a polygenic determinism conferring partial and generally broad-spectrum resistance (Poland et al. 2009; Roux et al. 2014b). For this reason, the molecular mechanisms underlying QDR remain poorly understood. However, the recent cloning of a limited number of QDR genes underlying resistance quantitative trait loci (QTLs) revealed a broad range of molecular functions (Delplace et al. 2022; Demirjian et al. 2023a). Only a very few QDR genes encode NLRs (nucleotide-binding leucine-rich repeat receptors) identified as *R* genes in the context of qualitative resistance (Broglie et al. 2006; Staal et al. 2006; Fukuoka et al. 2014; Demirjian et al. 2023b). On the other hand, several QDR genes encode different types of receptors including receptor-like kinases (RKs), signaling components such as kinases, and diverse metabolic functions (Corwin and Kliebenstein 2017; Pilet-Nayel et al. 2017; Nelson et al. 2018). This diversity of molecular functions together with the partial resistance conferred by QDR genes suggests that QDR results from a complex network integrating diverse pathways in response to multiple pathogenic determinants (Roux et al. 2014b). This suggests in turn that (i) individual QDR genes may confer resistance to multiple pathogens (Nelson et al. 2018; Kanyuka and Rudd 2019), and (ii) multiple receptors act together to perceive diverse pathogen determinants (Ngou et al. 2022). However, a limited number of receptors have been identified in the context of QDR in various plant–pathogen interactions.

In plants, RKs play an essential role in environmental signal perception, including pathogen detection at early stages of infection. RKs detect different pathogen epitopes. The transmembrane RK FLAGELLIN SENSING 2 (FLS2) is implicated in the detection of flg22, a conserved peptide of bacteria flagellin (Gómez-Gómez and Boller 2000; Bauer et al. 2001). The EF-Tu receptor (EFR) is involved in the perception of the peptide elf18, the N-terminal peptide of EF-Tu (Kunze et al. 2004; Zipfel et al. 2006). However, the number of distinct perception systems with specificity for microbe-associated molecular patterns (MAMPs) is difficult to estimate and a limited number of RKs have been described to recognize pathogen signatures (Tang et al. 2017). Recently, a complex and dynamic network of leucine-rich repeat (LRR)-RKs interactions has been described in Arabidopsis (Smakowska-Luzan et al. 2018). The association of LRR-RKs in heterodimers might

Received July 8, 2024. Accepted October 21, 2024.

participate in a large detection of diverse epitopes involved in various plant processes. RK-dependent recognition events converge into receptor hubs and overlapping immune signaling components can be recruited (Holton et al. 2015; Adachi and Tsuda 2019). These RKs take place in plasma membrane protein complexes including other RKs, receptor proteins (RPs), kinases, or pseudokinases (Boudeau et al. 2006; Monaghan and Zipfel 2012) and play a central role in the modulation of plant immunity. Some pathogen effectors have been shown to physically interact with essential signaling components to inhibit fast information spreading (Ahmed et al. 2018). In the same vein, complex associations between some NLRs have been observed in homodimers and heterodimers (Wróblewski et al. 2018; Contreras et al. 2023), and most cell surface and intracellular immune receptors appear to engage other receptors including ligand-binding receptors and transducer co-receptors (Wu et al. 2018). In summary, pathogen detection is not limited to a ligand perception event and receptors are organized in complex networks involving multiple perception events, in order to recognize a large variety of pathogen determinants. However, only a few of such ligand-binding receptors or receptor complexes have been identified and reported in the literature.

In the plant—pathogen interaction between *Arabidopsis thaliana* and the vascular bacterium *Xanthomonas campestris* pv. *campestris* (*Xcc*), RKS1 was identified to confer QDR to *Xcc* (Huard-Chauveau et al. 2013). RKS1 encodes an atypical kinase lacking some critical domains in the kinase catalytic core (Huard-Chauveau et al. 2013; Roux et al. 2014a). Atypical kinases (or pseudokinases) have been described as important regulators of signaling networks (Blaum et al. 2014; Reiterer et al. 2014). Recently, we reported a highly interconnected and decentralized RKS1-dependent protein–protein network, which is largely distinct from effector-triggered immunity (ETI) and pattern-triggered immunity (PTI) responses already characterized in *A. thaliana* (Delplace et al. 2020). From this network, we identified a signaling subnetwork that includes RKs not previously described in the context of plant immunity for most of them. Thus, functional analysis of RKs associated with RKS1 could provide a powerful tool for deciphering molecular mechanisms involved in the early signaling events of QDR. In this study, we report that the LRR-RK MDIS1-interacting receptor-like kinase 2 (MIK2) interacts with RKS1 and that MIK2 and RKS1 co-localized at the plasma membrane. We also show that *mik2* mutants exhibit an increased susceptibility to *Xcc* as compared to the wild type and that MIK2 catalytic activity is required for QDR to *Xcc*. In addition, the double mutant *mik2-1/rks1-1* showed a similar level of resistance against *Xcc* than the single mutants, indicating that they probably belong to the same pathway. Interestingly, MIK2 was recently demonstrated as a serine-rich endogenus peptide (SCOOP) perceiving RK (Hou et al. 2021; Rhodes et al. 2021). Accordingly, we found that MIK2 is positioned in a putative receptors-interacting network. Insertional mutants for some of these RKs showed increased susceptibility to *Xcc*, suggesting that they participate with MIK2 to *Xcc* perception. Our data support the hypothesis that MIK2 and RKS1 act as a scaffolding hub in an RK network to centralize and modulate pathogen determinant perception for QDR signaling and activation.

Results

RKS1 physically interacts with the kinase domain of MIK2

Using a yeast two-hybrid screen and a mutated version of RKS1 ($RKS1^{D191A}$) as a bait against a cDNA library generated from leaves inoculated by the strain *Xcc147* (Froidure et al. 2010), we identified among 43 candidate proteins (Delplace et al. 2020), a fragment of the kinase domain of MIK2 as a putative interactor of RKS1. We investigated the interaction between RKS1 and MIK2 using several strategies. First, to test whether RKS1 and MIK2 might be localized in the same cellular compartment, constructs using the fluorescent C-terminal tags eGFP and mRFP1, respectively, fused to the full-length sequences of $RKS1^{D191A}$ and MIK2, were co-transfected into Arabidopsis seedlings. As previously reported (Delplace et al. 2020), $RKS1^{D191A}$-eGFP was detected in the plasma membrane, the cytoplasm, and the nucleus. MIK2 was detected only in the plasma membrane (Fig. 1A). An overlap between eGFP and mRFP1 signals indicates a close subcellular localization of MIK2 and RKS1 in the plasma membrane. Second, co-immunoprecipitation assays were conducted using $RKS1^{D191A}$ fused to a c-myc tag and the kinase domain of MIK2 (MIK2-KD, amino acids 775 to 1045, including the cDNA fragment identified in Y2H) fused to a HA (Hemagglutinin) tag. After immunoprecipitation with an anti-HA antibody, $RKS1^{D191A}$-c-myc was detected when incubated with MIK2-KD-HA (Fig. 1B). ZAR1-HA, used as a positive control of interaction with RKS1 (Wang et al. 2015) and $RKS1^{D191A}$-c-myc, was not detected after immunoprecipitation with tag-HA, indicating the specific nature of interaction between MIK2 and RKS1 (Fig. 1C). An immunoprecipitation of $RKS1^{D191A}$-HA with an anti-HA antibody was also able to pull down MIK2 full-length protein with a c-myc tag (Supplementary Fig. S1). Third, we performed bimolecular fluorescence complementation (BiFC) assays using the split YFP system. The N-terminal half of the yellow fluorescent protein was fused to $RKS1^{D191A}$ and the YFP C-terminal was fused to *MIK2*, *ZAR1*, or *MtLYK3* (Lefebvre et al. 2010). When $RKS1^{D191A}$*-nYFP* was co-transformed with *MIK2-cYFP*, YFP signals were observed in the plasma membrane in *N. benthamiana* leaves. Similar signals were observed in *A. thaliana* protoplasts, localized exclusively at the cell periphery and excluding chloroplasts (Supplementary Fig. S2). As a comparison, when *RKS1-nYFP* was co-transformed with *ZAR1-cYFP*, YFP signals were detected in the plasma membrane and the cytoplasm (Fig. 1D). An extremely weak YFP signal was observed in the plasma membrane with $RKS1^{D191A}$-nYFP and the receptor MtLYK3-cYFP co-transformed in *N. benthamiana* leaves. Similar weak YFP signal was observed using co-transformation with the receptor MtLRRII-cYFP (Lefebvre et al. 2010) (Supplementary Fig. S3). These results collectively demonstrate that RKS1 is able to physically interact with the kinase domain of MIK2 in the plasma membrane.

MIK2 partially controls *RKS1*-dependent QDR

To investigate the function of *MIK2* in *Xcc* resistance, we characterized two T-DNA homozygous mutant lines for *MIK2*, i.e. *mik2-1* (GK-208H02, *mik2-3* in Coleman et al. 2020) and *mik2-2* (SALK_061769, *mik2-1* in Rhodes et al. 2021) (GABI-Kat and SALK collection, Col-0 background). The flanking regions of the T-DNA insertion sites were sequenced and the T-DNA insertion sites were found in the first exon of *MIK2*, at +2015 bp and +2644 bp, respectively (Fig. 2A). Complementarily, we generated transgenic lines complemented by *AtMIK2* in the *mik2-1* mutant background. *MIK2* gene expression in *mik2* mutants and *mik2-1* complemented lines is presented in Supplementary Fig. S4. While 31% and 5% of residual *MIK2* gene expression were found in *mik2-1* and *mik2-2* mutants, respectively, *MIK2* gene expression was restored in the complemented *mik2-1(35S::MIK2)* #1 and #2 lines (629% and 57%), as compared to Col-0. *mik2* mutants and *mik2-1* complemented lines

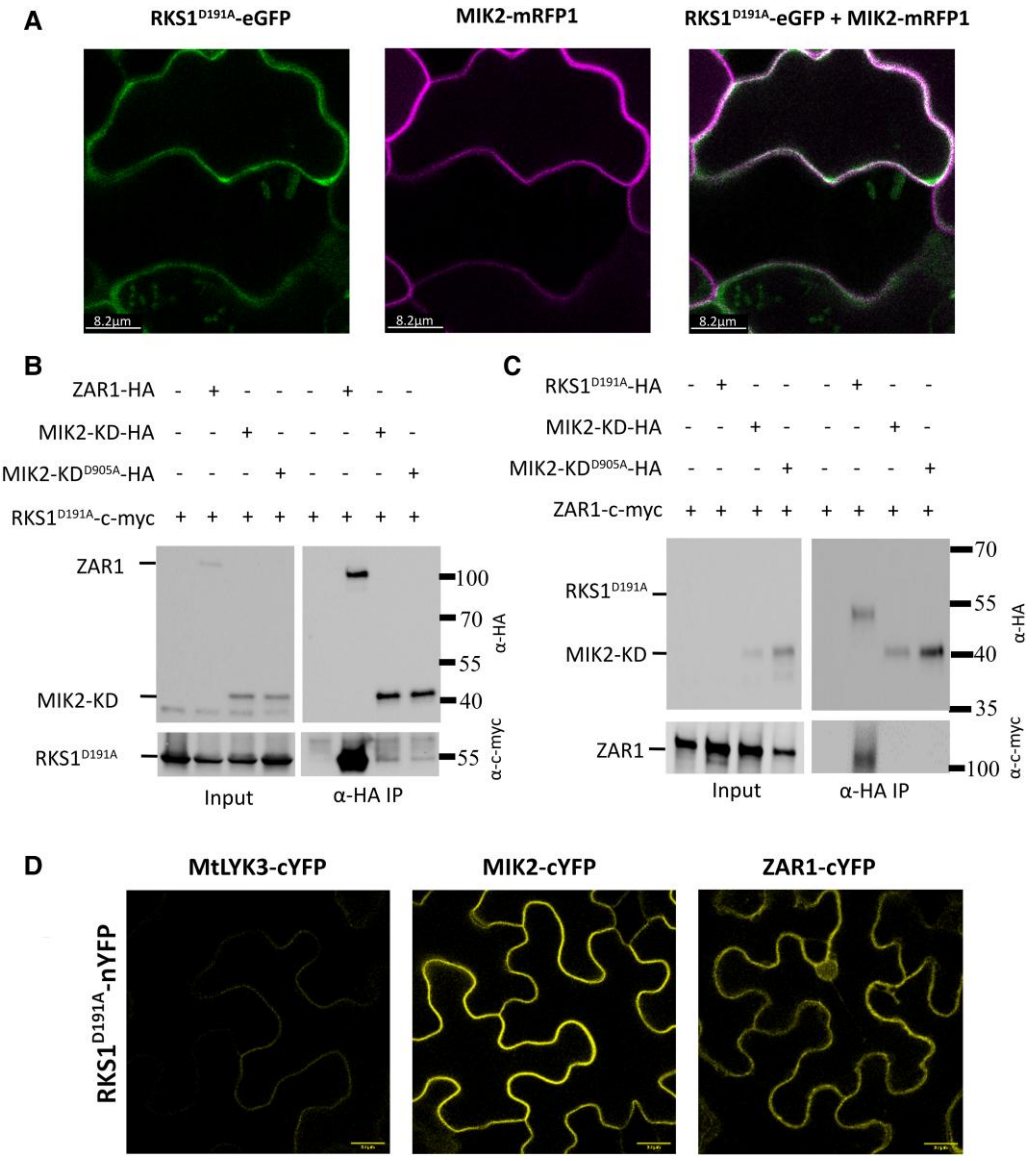

Figure 1. MIK2 physically interacts with RKS1 in the plasma membrane but not with ZAR1. **A)** Arabidopsis leaves were co-transformed by RKS1^{D191A}-eGFP and MIK2-mRFP1 full length constructs. Green corresponds to GFP signal, purple corresponds to RFP signal and white, co-localization between GFP and RFP. The white bars represent the ladder scale. **B)** Co-immunoprecipitation experiments with protein extracts from *N. benthamiana* inoculated with the C58C1 *Agrobacterium* strain carrying *ZAR1-HA*, *MIK2-KD-HA* or *MIK2-KD*^{D905A}-HA constructs, and with the C58C1 strain carrying *RKS1*^{D191A}*-c-myc*. Input proteins were extracted and revealed by anti-HA and anti-c-myc HRP immunoblotting. Then, total proteins were subjected to anti-HA immunoprecipitation (α-HA IP), separated on a 4%–15% SDS-PAGE gel and detected by anti-HA and anti-c-myc immunoblotting. **C)** Co-immunoprecipitation experiments with protein extracts from *N. benthamiana* inoculated by the C58C1 *Agrobacterium* strain carrying RKS1^{D191A}-HA, MIK2-KD-HA or MIK2-KD^{D905A}-HA constructs in one hand, and in the other hand, with a strain carrying ZAR1-c-myc. Proteins were analyzed by immunoblotting as described in part **B)**. **D)** BiFC assay between RKS1 and MIK2, ZAR1, or MtLYK3. RKS1^{D191A} was fused to nYFP and MIK2, ZAR1, and MtLYK3 were fused to cYFP. The indicated constructs were co-transformed into *N. benthamiana* leaves. The panel represents the YFP signal; bars in bottom right corner indicate the scale (20 µm).

were then inoculated with a bacterial suspension of the strain *Xcc568* and disease index evaluated at 3-, 5-, 7-, and 10-days post-inoculation (Fig. 2B and C; Supplementary Fig. S5). *mik2* mutants showed a significant increased susceptibility compared to Col-0, and this increased susceptible phenotype was not statistically different from the *rks1-1* mutant phenotype. These results were confirmed by measurement of *Xcc568* bacterial growth in planta (Supplementary Fig. S6). Complemented lines showed a similar resistance level than Col-0. These data confirm the implication of *MIK2* in QDR to *Xcc568*.

To further explore the respective roles of *MIK2* and *RKS1* in the QDR, we generated the double mutant *rks1-1/mik2-1* and phenotyped it in response to inoculation with *Xcc568* (Fig. 3A and B; Supplementary Fig. S6). The double mutant was significantly more susceptible than Col-0, slightly more susceptible than the single mutants, and less susceptible than the susceptible reference accession Kashmir-1 (Kas-1). This result suggests that *MIK2* might at least be partially involved in the *RKS1* pathway mediating QDR to *Xcc568*. To investigate more precisely the respective roles of *MIK2* and *RKS1* in these pathways, we analyzed the gene expression of a total of 36 genes highly connected to RKS1 from the previously reconstructed *RKS1*-dependent gene network (Delplace et al. 2020) or described to be dependent from *MIK2* expression (Hou et al. 2021). Expression of these genes was measured by

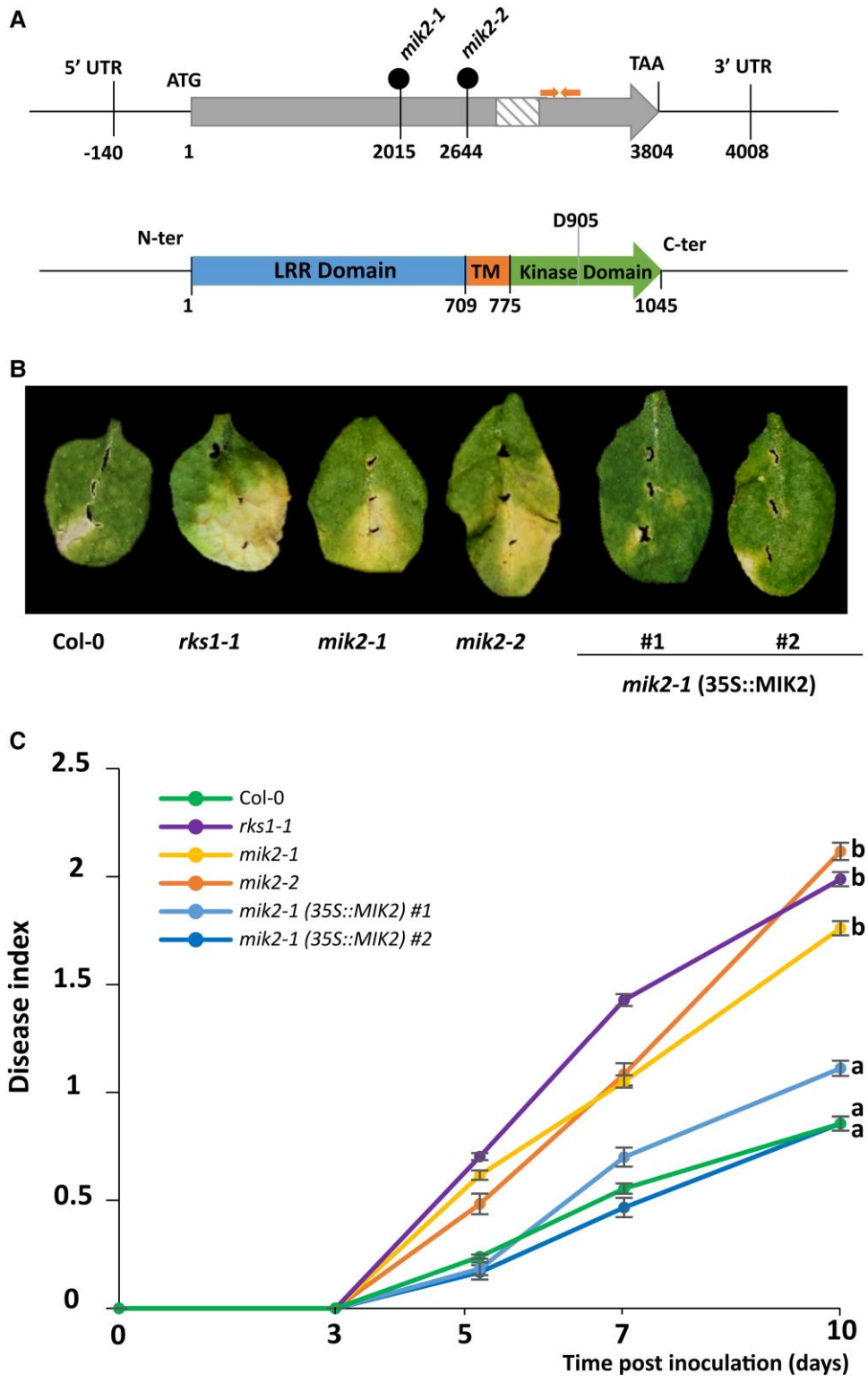

Figure 2. *Mik2* mutants are more susceptible to *Xcc568* inoculation. **A)** Schematic representation of the genomic organization of the *mik2* mutants and of the MIK2 protein. *MIK2* consists in two exons (gray boxes) and one intron (hatched box). For *mik2-1* and *mik2-2*, the T-DNA is integrated in the first exon, respectively at the position 2015 and 2644. The orange arrows indicate the primers used for measurement of *MIK2* gene expression. For the schematic representation of the MIK2 protein, blue represents the LRR domain; orange, the transmembrane domain; green, the kinase domain and D905 the aspartic amino acid involved in the kinase catalytic site. **B)** Disease symptoms were observed on leaves of *mik2* and *rks1* mutants, two *mik2-1* complemented lines with a *35S::MIK2* construct (#1 and #2) and Col-0 wild-type plants, 10 days postinoculation with a bacterial suspension adjusted to 2.10^8 cfu/mL. Images were digitally extracted for comparison. **C)** Time course evaluation of disease index after inoculation of *rks1-1* (purple), *mik2-1* (yellow), *mik2-2* (orange), *mik2-1 (35S::MIK2) #1* (light blue), *mik2-1 (35S::MIK2) #2* (dark blue), and the wild type Col-0 (green) with *Xcc568* under the same conditions as **B)**. Means and standard error of the mean (SEM) were calculated from 5 plants, 4 leaves/plant, and based on 3 independent experiments (60 values by point). Statistical tests were performed by comparing the disease index kinetics modeling differences, with a *P*-value threshold of 0.05. Different letters indicate significant differences in disease index kinetics among the lines.

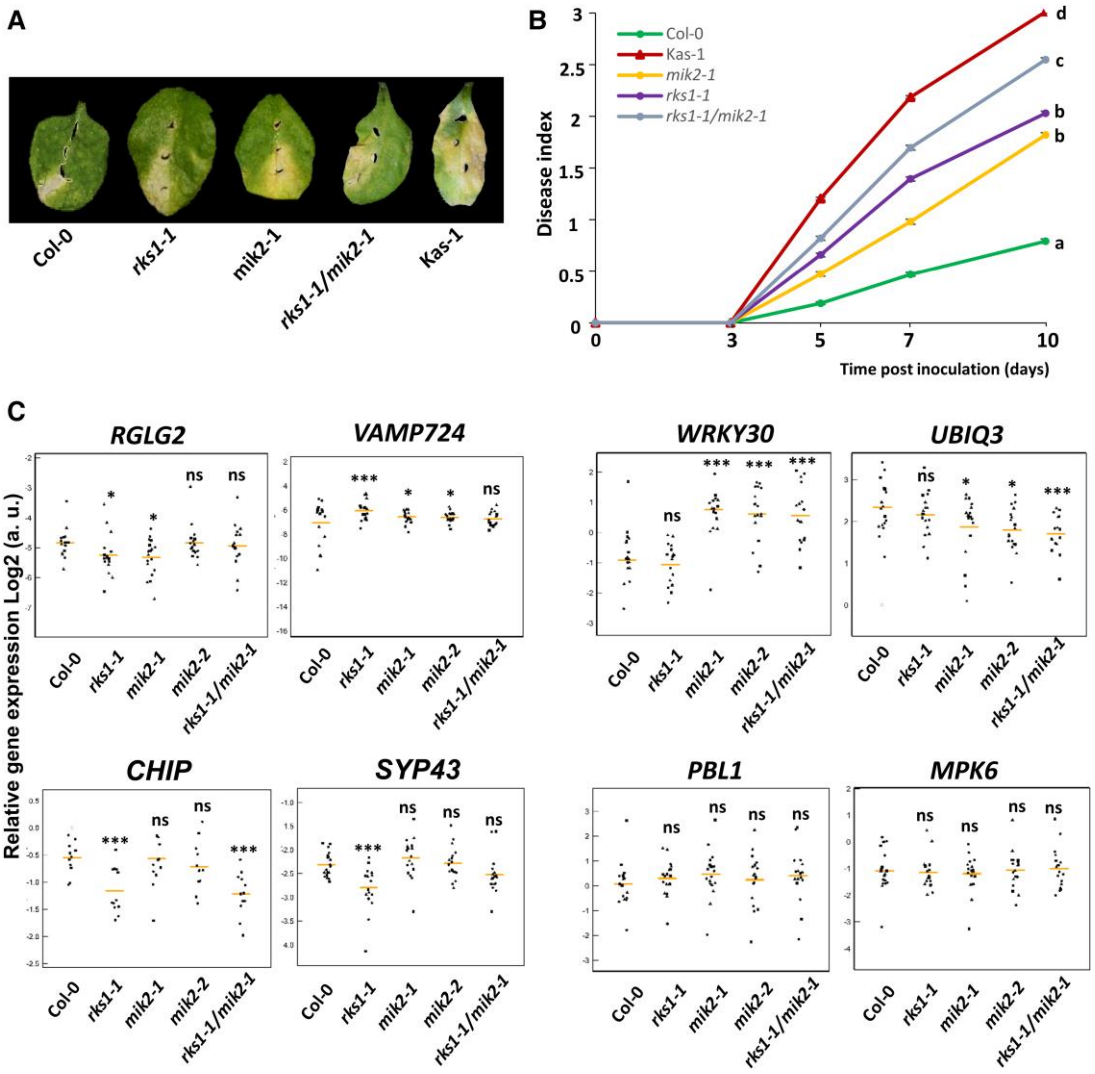

Figure 3. *MIK2* participates to the *RKS1* dependent control of QDR in response to *Xcc*. **A)** Disease symptoms were observed on leaves of *mik2-1* and *rks1-1* mutants, the double mutant *rks1-1/mik2-1*, the susceptible accession Kas-1 and the wild-type Col-0, 10 days after inoculation with a bacterial suspension of *Xcc568* adjusted to 2.10^8 cfu/mL. Images were digitally extracted for comparison. The Col-0 and *mik2-1* images are the same as those in Fig. 2B. **B)** Time course evaluation of disease symptoms and index after inoculation of *mik2-1* (yellow), *rks1-1* (purple), *rks1-1/mik2-1* (gray), the susceptible accession Kas-1 (red), and the wild type Col-0 (green) with a bacterial suspension of *Xcc568* adjusted to 2.10^8 cfu/mL. Disease scores were observed at 3-, 5-, 7-, and 10-days post-inoculation. Means and SEM) were calculated from five plants based on six independent experiments (120 values by point). Statistical tests were performed by comparing the disease index kinetics modeling differences, with a P-value threshold of 0.05. Different letters indicate significant differences in disease index kinetics among the lines. **C)** Jitter plots illustrating RT-qPCR results of the expression profile of genes from the RKS1-dependent gene network (Delplace et al. 2020), 6 h after inoculation with *Xcc568* (2.10^8 cfu/mL) in leaves of the wild type accession, Col-0, in *mik2-1* and *mik2-2* mutants, the *rks1-1* mutant and *rks1-1/mik2-1* double mutant. Dots correspond to the relative gene expression values adjusted for differences between the two experiments. Dots correspond to the relative gene expression values adjusted for micro-environmental variation between experiments by retrieving the residuals after fitting a model only with the term "experiment" and then adding the general mean value of relative gene expression values to these residuals. Data from the first, second, and third experiments are represented by square, circle, and triangle symbols. Mean relative gene expression is represented by an orange segment. The *RGLG2* and *VAMP724* genes present an expression profile dependent on the presence of *MIK2* and *RKS1*. The *WRKY30* and *UBIQ3* genes present an expression profile dependent on the presence of *MIK2* and independent of *RKS1*. The *CHIP* and *SYP43* genes present an expression profile independent of the presence of *MIK2* and dependent on *RKS1*. The *PBL1* and *MPK6* genes present an expression profile independent of the presence of *MIK2* and *RKS1*. Tests for statistical differences with Col-0 were performed with a GLM procedure in the *R* environment on three independent experiments with six plants/line/experiment. ns: nonsignificant, * $P < 0.05$, ** $P < 0.01$, *** $P < 0.001$. A correction for the number of tests was performed to control the FDR at a nominal level of 5%. a. u., arbitrary units.

RT-qPCR in Col-0 and the mutants *rks1-1*, *mik2-1*, *mik2-2*, *rks1-1/mik2-1*, 6 h after inoculation by *Xcc568* (Supplementary Table S1). A significant fraction of genes (44%) showed an expression dependent of the mutation *mik2* (either *mik2-2*, or both *mik2-1* and *mik2-2*). In this fraction, 31% showed an expression profile dependent of both mutations *rks1* and *mik2*. Several examples are presented in Fig. 3C. These results clearly support the hypothesis that *MIK2* and *RKS1* initiate common signaling pathways to control gene expression. However, these common pathways appear to constitute only a fraction of the ones initiated by both proteins, in good agreement with the double mutant phenotype reported in Fig. 3A and B. Interestingly, *MIK2* gene expression was significantly reduced in two independent *RKS1* overexpressing lines (*RKS1-OE1* and *RKS1-OE2*) (Huard-Chauveau et al. 2013; Delplace et al. 2020) (Supplementary Fig. S4B), suggesting that *MIK2* gene expression might be regulated by an overexpression of *RKS1*.

Catalytic activity of MIK2 is required for QDR to *Xcc568*

Taking in account that (i) MIK2 participates to the *RKS1* dependent QDR in response to *Xcc*, and (ii) RKS1 interacts with the kinase domain of MIK2, we tested whether these MIK2 functions depend on its kinase catalytic activity. For this purpose, an inactive catalytic mutant version of MIK2 full-length protein, MIK2^{D905A}, affected in the putative active HRD site of the MIK2 kinase domain, was generated. Kinase assays using MIK2 and MIK2^{D905A} showed that MIK2 was able to autophosphorylate and that the aspartic acid residue in position 905 was required for MIK2 autophosphorylation activity (Fig. 4A). First, the catalytic mutated version of the kinase domain of MIK2, MIK2-KD^{D905A}-HA, was able to interact with RKS1^{D191A} fused to the c-myc tag, as shown for the wild type version of MIK2 (Fig. 1). After immunoprecipitation with an anti-HA antibody, RKS1^{D191A}-c-myc was detected when incubated with MIK2-KD^{D905A}-HA (Fig. 1B), indicating that the aspartic acid residue of the HRD motif of MIK2 is not required for the RKS1-MIK2 interaction. Furthermore, incubation of MIK2 and MIK2^{D905A} protein with RKS1 or RKS1^{D191A} did not reveal MIK2 or RKS1 phosphorylation activities in vitro (Fig. 4A). Second, after introduction of MIK2^{D905A} into the *mik2-1* mutant for a complementation test, three transgenic lines were characterized and inoculated with *Xcc568*. The three complemented lines showed significant phenotypic differences from Col-0, but similar phenotypes to the *mik2-1* mutant (Fig. 4B and C). MIK2^{D905A} version was therefore not able to restore resistance in the *mik2-1* mutant at a similar level as the wild type. These results indicate that the catalytic activity of MIK2 is required to confer QDR to *Xcc568*. Finally, transgenic lines overexpressing *MIK2* or *MIK2*^{D905A} in Col-0 were also characterized (Fig. 4D). *MIK2* expression was increased in 35S::MIK2 lines (517% and 161% in the two lines compared to Col-0) and reduced in 35S::MIK2^{D905A} lines (26% and 42% in the two lines compared to Col-0) probably because native *MIK2* was silenced in these lines (Supplementary Fig. S4). Inoculation tests of these lines revealed that MIK2 and *MIK2*^{D905A} mis-expression in Col-0 did not significantly affect resistance to *Xcc568*, with the exception of one line, Col-0 (35S::MIK2) #2, which a slight reduction of resistance to *Xcc568* was observed (Fig. 4D).

MIK2 and RKS1 take place in an RK network

We demonstrated that MIK2 and RKS1 form a complex that is involved in QDR to *Xcc*. It is now tempting to speculate, given (i) our results showing that these two proteins share only a part of their downstream signaling pathways, and (ii) the RKS1 dependent network previously identified (Delplace et al. 2020) that these two proteins do not act isolated and require other perception/signaling proteins to orchestrate QDR. To test this hypothesis, we first identified from the literature, proteins physically interacting with MIK2 (demonstrated or putative interactions, Dataset 1). A MIK2-centralized network was reconstructed including 25 RKs, BSK3, and RKS1. Nine and five RKs interacting with MIK2 were described in the literature to be involved respectively in plant immunity (Kemmerling et al. 2007; Blaum et al. 2014; Mata-Pérez et al. 2015; Liu et al. 2016; Yeh et al. 2016; Mendy et al. 2017; van der Burgh et al. 2019; Chan et al. 2020; Laohavisit et al. 2020) and plant development (Takeuchi and Higashiyama, 2016; Wang et al. 2016; Duckney et al. 2017; Crook et al. 2020). Interestingly, 7 proteins from the RKS1 dependent protein–protein network were found highly connected to the MIK2-centralized network (Fig. 5A). Given that (i) proteins with an extracellular domain (ECD) length up to 400 amino acids may act as putative co-receptors, and (ii) proteins with a larger ECD may act as putative ligand recognition receptors (Xi et al. 2019), this network is composed of 25 RKs described with a structure indicative of ligand binding perception proteins (including MIK2) and 12 co-receptors possibly implicated in signal transduction events (Fig. 5B).

To evaluate the possible implication of some of the MIK2-RKS1 network components in QDR to *Xcc*, 17 mutants (corresponding to 16 genes) were collected and characterized for their response to *Xcc568*. The phenotypic data are summarized in Fig. 5C to E. Eight mutants corresponding to seven receptors showed a strong alteration in their response to *Xcc568* (at least 30% of increased susceptibility), compared to Col-0, while mutants corresponding to seven other receptors showed a weak alteration (Fig. 5D and E) (Supplementary Tables S2 and S3). Interestingly, mutants showing a strong alteration correspond to network components known to operate in plant immunity, while the mutants with a weak effect correspond to components associated with plant development or without known function. Because MIK2 was recently proposed to operate by sensing cell wall perturbations (Van der Does et al. 2017), we also phenotyped several cell wall integrity altered mutants, i.e. *herk1*, *the1-4*, and *FER* (Cheung and Wu 2011; Nissen et al. 2016), in response to inoculation with *Xcc* (Supplementary Fig. S7). The *herk1-1* and *the1-4* mutants did not show a significantly altered response to *Xcc568*, while *fer5* mutants were slightly more resistant than Col-0. Our data suggest that the genes *HERK* and *THE1* are not significantly involved in QDR to *Xcc*. In addition, mutants for *MIK2-like*, the closest homolog of *MIK2* (60% AA identity), and for *MIK1*, a receptor also interacting with the Male Discoverer 1 receptor, show only weak alteration in response to *Xcc* (Supplementary Fig. S7). Taken together, these results indicate that at least seven RKs, highly connected to MIK2 and/or RKS1, have a partial effect in QDR to *Xcc568*. These findings reveal the complexity of the molecular mechanisms involved in MIK2/RKS1-dependent signaling pathways, in good agreement with the genetic and molecular complexity of QDR.

Discussion

Even if QDR is the most prevalent form of resistance in natural populations and crop fields, the identification of genes involved in the molecular mechanisms underlying QDR is still in its early stages (Roux et al. 2014b; French et al. 2016). In this study, we have identified the LRR receptor kinase MIK2 as an interactor of RKS1, a major determinant of QDR to the bacterial pathogen *Xcc* (Huard-Chauveau et al. 2013; Delplace et al. 2020). In addition, we found that MIK2 plays a role in QDR to *Xcc*, depending on its kinase catalytic activity. Taking into account (i) the RKS1-dependent network previously identified (Delplace et al. 2020), and (ii) the ability of MIK2 to interact with diverse RKs (receptors and co-receptors, Xi et al. 2019), themselves involved in interaction with RKS1 protein partners, our results suggest a role for the complex MIK2-RKS1 as a scaffolding hub in a RK network to modulate Xanthomonas determinant perception for QDR signaling and activation. The functional relevance of this RK network, centered on the MIK2-RKS1 complex, has been addressed by mutational analysis, thereby revealing the involvement of several RK components in QDR regulation. While the molecular mechanisms underlying QDR remain poorly characterized, combining functional validation, protein–protein interaction analysis, and network reconstruction, revealed insights into a perception system that regulates QDR in response to *Xcc*.

The cell surface receptor-like kinase MIK2 interacts with RKS1 to activate QDR

By using the yeast two-hybrid system, we previously identified 43 proteins as putative interactors of RKS1, including 21 metabolism-

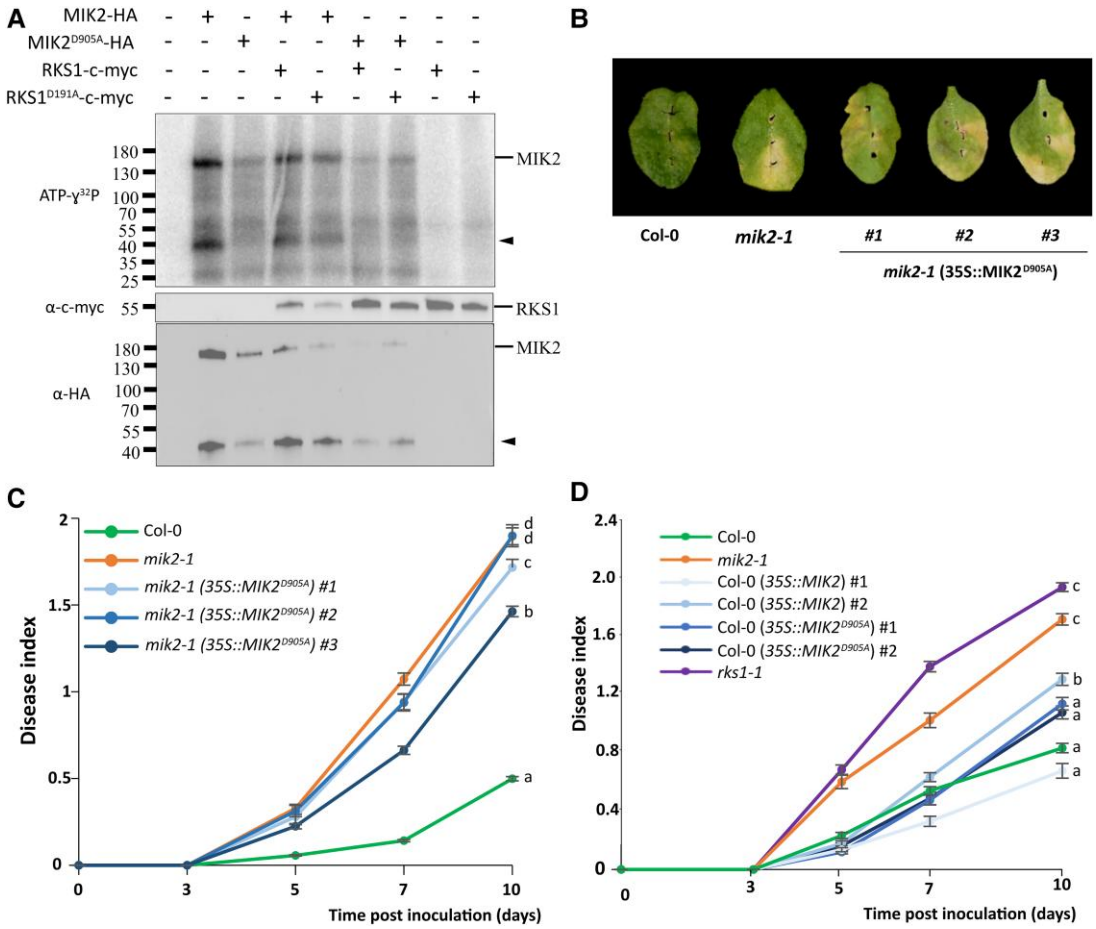

Figure 4. The catalytic activity of MIK2 is required for resistance to *Xcc568* but overexpression of MIK2 and MIK2^{D905} in Col-0 does not increase resistance to *Xcc568*. **A)** Kinase assay with protein extracts from *N. benthamiana* leaves transformed by Agrobacterium carrying the constructs MIK2-HA, MIK2^{D905A}-HA, RKS1-c-myc, or RKS1^{D191A}-c-myc. The total protein extracts were subjected to anti-HA or anti-c-myc immunoprecipitation. The immunoprecipitated proteins were incubated for 2 h at room temperature with ATP-γ^{32}P. The proteins were separated on a 4%–15% SDS-PAGE gel and detected by anti-HA, anti-c-myc immunoblot, and the presence of ATP-γ^{32}P by autoradiography. Black triangles indicate the potential MIK2 kinase domain, probably cleaved due to the protein extraction procedure. **B)** Disease symptoms were observed on leaves of *mik2-1* mutant, three *mik2-1* complemented lines with a 35S::MIK2^{D905A} construct and wild-type plants, 10 days postinoculation with a bacterial suspension of *Xcc568* adjusted to 2.10^8 cfu/mL. Images were digitally extracted for comparison. The *mik2-1* image is the same as the one in Fig. 2B. **C)** Time course evaluation of the disease index of *mik2-1* mutant (orange), three *mik2-1* complemented lines with a 35S::MIK2^{D905A} construct (blue) and wild-type plants (green) after inoculation with *Xcc568* under the same conditions as **A)**. Means and SEM were calculated from 5 plants per line per experiment and based on 3 or 4 independent experiments (60 to 80 values by point). Statistical tests were performed by comparing the disease index kinetics modeling differences, with a *P*-value threshold of 0.05. a, b, c, or d represent statistical groups based on comparison of disease index kinetics. **D)** Time course evaluation of the disease index of lines overexpressing *MIK2* or *MIK2*^{D905A} in Col-0 (35S promoter construction), *rks1-1* and *mik2-1* mutants and the wild type plants inoculated with a bacterial suspension of *Xcc568* adjusted to 2.10^8 cfu/mL. Means and SEM were calculated from 5 plants per line and based on 3 independent experiments (60 values by point). a, b, or c represent statistical groups based on comparison of disease index kinetics performed as in **D)**.

related proteins and 6 signaling-related components (ex: EFR, KIN11, SGT1a, MKP1, RANBP1, and NLP7) (Delplace et al. 2020). Here, we demonstrated the interaction between RKS1 and the kinase domain of the receptor-like kinase MIK2. Co-localization and BiFC experiments confirmed the subcellular localization of the two proteins and their interaction in the plasma membrane. Interestingly, RKS1 is localized in the plasma membrane, cytoplasmic tracks, and the nucleus (Delplace et al. 2020), suggesting different functions for RKS1 including a contribution to pathogen perception events. The NLR ZAR1 was demonstrated to form a complex with RKS1 in the cytoplasm to perceive the injected effector AvrAC from *X. campestris* (Adachi et al. 2019; Wang et al. 2019). The interaction of RKS1 with a receptor-like protein such as MIK2, suggests that RKS1 might also be involved in the extracellular perception of pathogen determinants or endogenous peptides at the plasma membrane. Based on our findings, RKS1 might be part of membrane complexes that, similarly to MIK2, include cell surface receptors required for transduction events (Antolín-Llovera et al. 2012). RKS1-receptor complexes may be dynamic, depending on the nature of the pathogen. Similar to the pseudokinase domain of the receptor BIR2 involved in the allosteric regulation of the receptor BAK1 (Blaum et al. 2014), the RKS1-MIK2 complex, MIK2 or RKS1, could act as a scaffolding protein complex and participate in the regulation of signaling pathways as a molecular switch, depending on the context of protein–protein interactions (Roux et al. 2014a; Murphy et al. 2017). Interestingly, MIK2 seems connected with multiple sensing systems including cell wall integrity sensing (CWIS) (Rhodes et al. 2021), root growth and response to abiotic and biotic stresses (Julkowska et al. 2016; Van der Does et al. 2017). In particular, MIK2 is involved in the perception of the phytocytokine peptide SCOOP12, by heterodimerizing with BAK1 (Rhodes et al. 2021). While no plant developmental function has

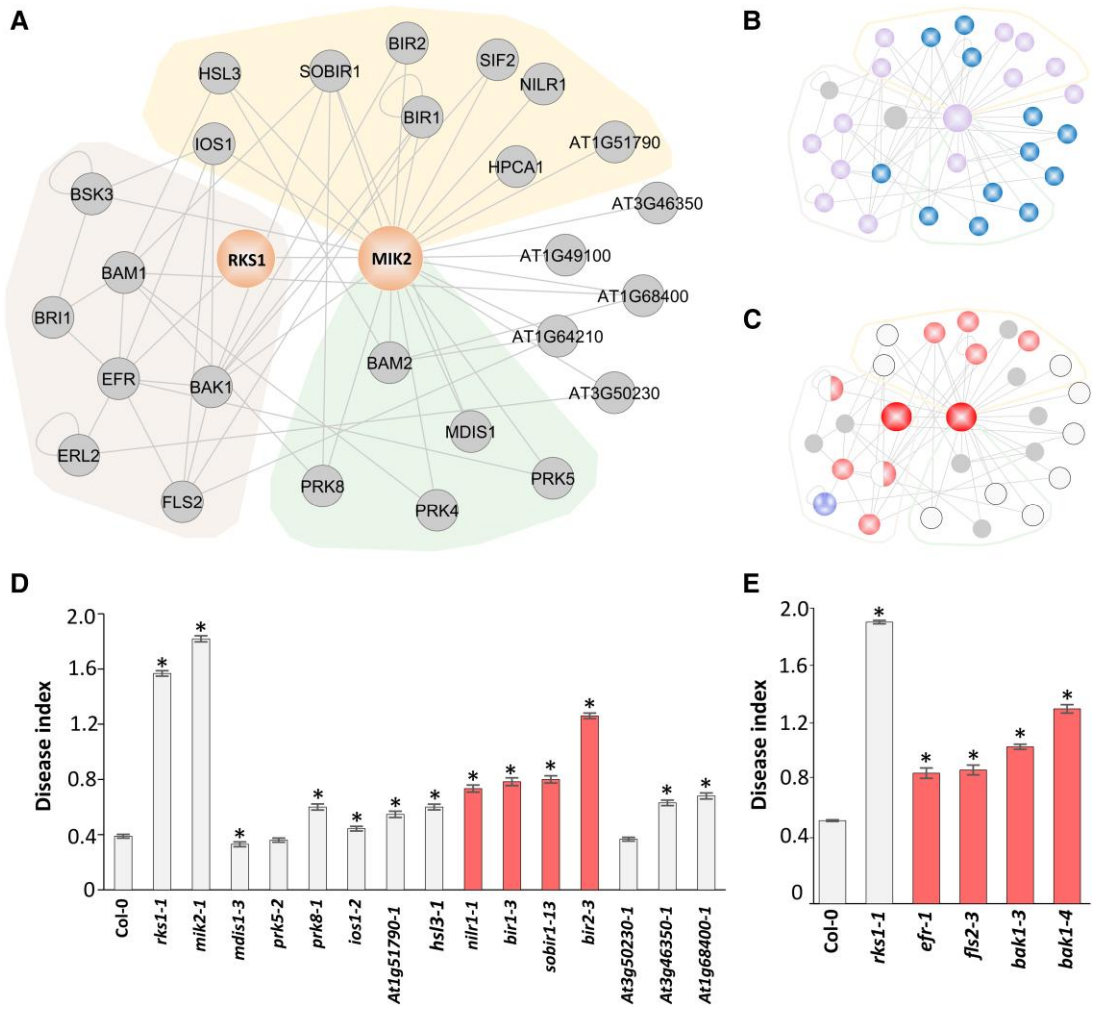

Figure 5. MIK2 and RKS1 as hubs of an RK network. **A)** MIK2 protein–protein interaction subnetwork was reconstructed from STRING and BioGrid databases and plotted with Cytoscape. The light brown area indicates proteins recovered from the RKS1 dependent network (Delplace et al. 2020). The yellow area indicates RKs interacting with MIK2 and described to play a role in plant immunity (Kemmerling et al. 2007; Blaum et al. 2014; Mata-Pérez et al. 2015; Liu et al. 2016; Yeh et al. 2016; Mendy et al. 2017; van der Burgh et al. 2019; Chan et al. 2020; Laohavisit et al. 2020). The green area indicates RKs interacting with MIK2 and described to be implicated in plant development (Takeuchi and Higashiyama, 2016; Wang et al. 2016; Duckney et al. 2017; Crook et al. 2020), the uncolored zone corresponds to hypothetical RKs. The gray lines between nodes indicate protein–protein interaction. **B)** In the MIK2 protein–protein interaction network, purple circles represent RKs from the "ligand perceiving group" (Xi et al. 2019), blue circles represent LRR-RKs from the "co-receptor group" and gray circles, other proteins. The gray lines between nodes indicate protein–protein interaction. The colored outlines represent function of proteins (light brown, proteins recovered from the RKS1 dependent network; yellow, RKs interacting with MIK2 and described to play a role in plant immunity; green, RKs interacting with MIK2 and described to be implicated in plant development). **C)** Each circle represents the phenotype of the mutant corresponding to the protein component of the network. Colored circles indicate some mutants significantly affected in their response to *Xcc*568. Mutants represented in red are significantly affected in their response to *Xcc* (at least 30% of increased susceptibility compared to Col-0 disease index), according to **D)** and **E)**, and those represented in purple are more resistant compared to Col-0 according to Delplace et al. (2020). The circle is divided according to the number of tested mutants. White circles correspond to mutants with a phenotype similar to the one of the wild type line. No mutant was tested for genes represented in gray. Data presented for ERL2 and BSK3 were recovered from Delplace et al. (2020). The gray lines between nodes indicate protein–protein interaction. The colored outlines represent function of proteins (light brown, proteins recovered from the RKS1 dependent network; yellow, RKs interacting with MIK2 and described to play a role in plant immunity; green, RKs interacting with MIK2 and described to be implicated in plant development). **D)** Disease index of mutants corresponding to genes belonging to the MIK2-RKS1 network, at 10 dpi after inoculation with a bacterial suspension adjusted to 2.10^8 cfu/mL. *Represents kinetic modeling difference with Col-0 time course, based on five independent experiments with 5 plants/mutant. Light gray bars correspond to mutants for RKs described in part **A)** and dark gray bars correspond to *rks1-1* mutant and Col-0 wild type used as controls. Mutants represented in red are significantly affected in their response to *Xcc* (at least 30% of increased susceptibility compared to Col-0 disease index). Statistical tests were performed by comparing the disease index kinetics modeling differences, with a *P*-value threshold of 0.05. Error bar represent SEM. **E)** Disease index at 10 dpi after inoculation in the same conditions as **D)**. *Represents kinetic modeling deference with Col-0 time course in 3 to 5 experiments with 5 plants/mutants. Light gray bars indicate mutants for RKs from the RKS1 dependent network and dark gray bars correspond to *rks1-1* mutant and Col-0 wild type used as controls. Mutants represented in red are significantly affected in their response to *Xcc* (at least 30% of increased susceptibility compared to Col-0 disease index). Statistical tests were performed by comparing the disease index kinetics modeling differences, with a *P*-value threshold of 0.05. Error bar represent SEM.

been suggested for RKS1 yet, it is a major determinant of QDR for which CWIS might be a component (Zuo et al. 2015; Bani et al. 2018). To test this hypothesis, mutants for CWIS (*herk1-1*, *the1-4*, and *fer-5*) were phenotyped in response to *Xcc*. None of the CWIS mutants was found more susceptible to *Xcc568* (Supplementary Fig. S7), suggesting that CWIS is not required to confer QDR to *Xcc*. These results show that CWIS does not generally interfere with QDR to *Xcc*, in opposition to a previous study proposing

that *MIK2* and *THE1* could function in the same pathways but distinct from the *FER* pathways, against *Fusarium oxysporum* (Coleman et al. 2020). This discrepancy might be explained by the fact that *F. oxysporum* is more of a root and cell wall invasive pathogen in comparison with the leaf vascular pathogen *Xcc* (Kubicek et al. 2014; An et al. 2020). MIK2 may participate in the detection of multiple ligands (Wang et al. 2016; Rhodes et al. 2021), that could require MIK2 directly, or MIK2 interacting with other ligand-perceiving receptors (Fig. 5B). In the future, to decipher the molecular dialogues between *Xcc* and host plants, a challenge would be to identify putative *Xcc* or/and plant cell damages derived ligands perceived by MIK2. To initiate this investigation into potential ligands perceived by MIK2 during *Xcc568* infection, we first examined the expression patterns of *PROSCOOPs* at early time points postinfection using RNA-seq data from Delplace et al. (2020). Indeed, as already mentioned, MIK2 has been found to be involved in the perception of the phytocytokine peptide SCOOP12, and PROSCOOP genes belong to a family encoding secreted propeptides, which are maturated in SCOOP peptides (Rhodes et al. 2021; Yang et al. 2023). Interestingly, 9 *PROSCOOPs* were found to share the same expression pattern as *MIK2* during infection, including a strong induction of *PROSCOOP12*, and, in total, at least 28 *PROSCOOPs* are induced between 0 and 6 h after *Xcc568* infection (Supplementary Fig. S8). Second, we identified a SCOOP-like motif in the XopAM protein from *Xcc568* (Supplementary Fig. S9), a putative MIK2 ligand that constitutes an interesting target for future work. Unlike other AvrE-T3Es, XopAM may function as a lipase in *N. benthamiana*, affecting membrane integrity and inducing cell death (Xie et al. 2023), potentially releasing XopAM into the apoplast where the SCOOP-like motif could be perceived by MIK2. However, the function of XopAM in the *Xcc*–plant interaction remains unclear. XopAM contains a translocation signal (Potnis et al. 2011) but is not located near the T3SS cluster, and type III secretion chaperone genes are not found adjacent to the gene encoding XopAM (Degrave et al. 2015). Thus, despite being part of the core type III secretome in multiple *Xcc* strains (Guy et al. 2013), its role as a T3E effector is unconfirmed, and its translocation via T3SS needs to be experimentally confirmed. In conclusion, endogenous SCOOPs and/or pathogen SCOOP-like peptide mimics, might play a critical role in the early perception of *Xcc* by MIK2 or MIK2 in association with other immune components, and represent promising putative actors of this interaction, similarly to nematode-encoded RALF peptide mimics reported to facilitate parasitism for example (Zhang et al. 2020). Approaches including physical protein-ligand interactions using MIK2 and other potential RKs identified in this study would help to shed some light on the perception events responsible for QDR. To conclude, *MIK2* with its diverse functions in CWIS and responses to abiotic and biotic stress could play different functional roles depending on its interacting partners. As a complex with RKS1, it appears to be a major player in plant immune responses to the bacterial pathogen *Xcc*.

RKS1-MIK2 as a regulatory complex for QDR signaling?

While receptor kinases, and among them the LRR-receptor kinases, constitute the largest protein kinase family in plants, a large part of these receptors and their putative interactors are still functionally uncharacterized. Here, we showed that *MIK2* confers QDR to *Xcc568* at a similar level as *RKS1*. Analysis of the double mutant *rks1-1/mik2-1* revealed that *MIK2* and *RKS1* probably act in a common pathway in response to *Xcc*, which might represent only a part of the immune response, as the double mutant express an intermediary phenotype, more susceptible than the resistant reference accession, less susceptible than the susceptible reference accession, but slightly more susceptible than the single mutants. To further explore their respective functions, we measured the expression of a set of 36 genes from the previously identified RKS1-dependent network (Delplace et al. 2020) or described to be dependent on *MIK2* (Hou et al. 2021). A major part of these genes (44%) showed an expression dependent on the mutation *mik2*. For this set of genes, 31% (including *RGLG2* and *VAMP724*, presented in Fig. 3) showed an expression profile dependent on both mutations *rks1* and *mik2*, confirming the existence of common pathways activated by both proteins. We observed that the reduced gene expression of *RGLG2* and *VAMP724* in *rks1-1* and *mik2-1*, which was rescued in *rks1-1/mik2-1*, suggesting a potential epistatic interaction between *MIK2* and *RKS1*, where one mutation restores expression affected by the second mutant. *RGLG2* was described as a RING domain ubiquitin E3 ligase implicated in stress drought adaptation and VAMP724 as SNAREs protein involved vesicle-associated trafficking (Yu et al. 2020; He et al. 2023). Eleven genes were found specifically dependent of *MIK2*, such as the transcription factor WRKY30, implicated in abiotic stress tolerance (Scarpeci et al. 2013). These different roles can be explained by the putative interactions of MIK2 with other signaling partners in plasma membrane receptor complexes (He et al. 2018). Together these data confirm the implication of *MIK2* and *RKS1* in QDR signaling, potentially via the MIK2 kinase domain. Indeed, we showed that MIK2, as classical RD (arginine and aspartic acid) RKs such as BAK1 and CERK1 (Oh et al. 2010; Suzuki et al. 2018), exhibits an autophosphorylation activity dependent on the aspartic acid 905 residue. Similar to BRI1 that is maintained in an inactive stage by autophosphorylation (Oh et al. 2012), MIK2 phosphorylation activity could be required for autoregulation. Surprisingly, the MIK2 aspartic acid 905 residue appeared not essential for RKS1 interaction. These results suggest, in agreement with the functioning of multiple plasma membrane receptor complexes (Burkart and Stahl 2017) that RKS1 might act as a scaffolder for receptor complex assembly in the context of QDR. A similar role was described for the PTI receptors FLS2 and EFR, with the FER scaffolding receptor (Stegmann et al. 2017). Our results are in good agreement with the recent "Invasion model" proposing that there might be no clear distinction between PTI, ETI, and more widely the different forms of plant immunity responses (Cook et al. 2015; Kanyuka and Rudd 2019) (including QDR), and that broad-spectrum immunity might depend on complex networks of cell surface immune receptors in most cases. Here, we extend this model by proposing that RKS1 participates in surface and intracellular perception mechanisms (in interaction either with MIK2 or ZAR1), which are initiated either in the apoplast or the cytosol.

MIK2/RKS1 complex as a hub to coordinate an RK perception network?

LRR-RKs sense a wide array of molecules produced exogenously or endogenously and regulate plant growth and immunity. They can operate in a regulatory network (Smakowska-Luzan et al. 2018) where small LRR-RKs (co-receptors) are involved (i) in fine-tuning (by activation or stabilization) of ligand binding receptors, and (ii) as regulatory scaffolds for the organization of the signaling network (Xi et al. 2019). In this context, understanding the functioning of the MIK2/RKS1 complex in QDR needs to be replaced within a protein–protein interaction (PPI) network. From the literature,

we identified MIK2 interacting proteins, and generated a network including, beyond RKS1, RKs from the RKS1 dependent network. MIK2, a ligand binding receptor, takes place in a highly connected RK network including signaling proteins involved either in immunity or plant development (Fig. 5). Interestingly, the MIK2-RKS1 network reveals no clear co-receptor hub (linked to ligand-perceiving receptors) such as BAK1 (Smakowska-Luzan et al. 2018). In addition, MIK2 is connected to diverse receptors and not only with co-receptors, such as the ligand-perceiving receptor BAM1 that forms a complex with several co-receptors of the CIK family (Cui et al. 2018). The MIK2-RKS1 centralized network appears more diverse than co-receptor and ligand perceiving receptor associations (Xi et al. 2019). This might be due to the dynamic complexity of the perception events involved in QDR, and probably also to the insufficient characterization or absence of some LRR-RKs (or other receptors) in this reconstructed network. A functional analysis of this network by mutant analysis showed that seven RKs are involved in QDR to *Xcc* with a strong effect (Fig. 5), described to be related to plant immunity and connected with MIK2 (BIR1, BIR2 NIRL1, SOBIR, EFR, FLS2, and BAK1) (Kemmerling et al. 2007; Blaum et al. 2014; Liu et al. 2016; Laohavisit et al. 2020; Rhodes et al. 2021). Among these RKs, the MIK2/RKS1 complex might recruit some RKs as a perception system to trigger QDR, similarly to the co-receptor BAK1. Interestingly, BIR2 plays a major positive regulatory role in QDR to *Xcc* (Fig. 5). BIR2 has previously been reported as a negative regulator of PTI in Arabidopsis (Halter et al. 2014a). Interaction with BAK1 in a kinase activity-dependent manner negatively controls the formation of complexes between BAK1 and specific ligand-binding receptors, to regulate plant immune responses (Halter et al. 2014b). More recently and in line with our findings, BIR2 has been found to positively regulate resistance to bacterial and oomycete pathogens in *N. benthamiana* (Liu et al. 2023), emphasizing a key role for this RK in immunity. Beyond BIR2, multiple RKs contribute quantitatively to resistance to *Xcc*, and the association of RKS1 with the kinase domain of different RKs suggests that RKS1 may act as a receptor platform regulating the formation of RK complexes with specific ligand-binding receptors. In this context, MIK2 plays a central role with RKS1, by perceiving multiple peptides/ligands (Wang et al. 2016; Rhodes et al. 2021) and by recruiting a diversity of co-receptors. The perception by RKs of multiple signals (MAMPs/DAMPs or effectors released during infection) could trigger diverse interconnected signaling pathways, where MIK2/RKS1 complex may potentiate different pathways, depending on the nature of the ligand perceived (Ngou et al. 2021). Thus, seven other RKs connected with MIK2, including co-receptors with unknown functions (*AT1G68400* and *AT1G64210*) or with plant developmental functions (MDIS1 and PERK8) are implicated in QDR to *Xcc* but to a much lesser extent, indicating that MIK2 in association with RKS1, could mainly recruit RKs involved in immune responses. Similar to the receptor BAK1 described to be a co-receptor for multiple LRR receptors involved in PTI and plant development (Postel et al. 2010; Zhou et al. 2019), MIK2 might require specific RKs or other signaling components to coordinate immunity and development perception systems. Interestingly, cytoplasmic kinases are also known as molecular switches between plant development and immunity pathways, such as BSKs (brassinosteroid kinases) (Lin et al. 2013). BSK3, which is implicated in brassinosteroid signaling, confers partial resistance to *Xcc* and thus can be a key regulatory compound in the MIK2/RKS1-centralized network (Sreeramulu et al. 2013; Delplace et al. 2020). In this line, BSK3 was also described as a scaffolding protein for plant development (Ren et al. 2019). Another interesting feature of this network is the presence of four RKs from the RKS1-dependent network: ERL2, BAK1, EFR, and FLS2. EFR and FLS2 are known to directly perceive pathogen determinants (Chinchilla et al. 2006; Zipfel et al. 2006) and can therefore participate in the perception of multiple pathogen determinants, which is in good agreement with the view of QDR as a complex network integrating diverse pathways in response to multiple pathogenic determinants (Roux et al. 2014b). While receptors could participate directly or indirectly to pathogen perception with strong implication in QDR to *Xcc*, such as BAK1 or BIR2, other receptors with a weak implication in QDR, like MDIS1 or IOS1, could have either redundant functions with other receptors or only an indirect implication in *Xcc* perception. In the future, consolidation of the PPI network, investigation of other possible interactions among the different components and testing whether the contribution of these RKs in resistance to *Xcc* depends on the presence of RKS1 or MIK2, will permit to confirm and extend the complexity of this network. Taken together, our results suggest that the RKS1/MIK2 complex in relation to a number of additional RKs might participate in a perception system and act as a scaffolder hub to coordinate the assembly of multiple perception complexes.

In summary, the MIK2/RKS1 complex takes place in an RK network in the plasma membrane and might be involved in the perception of multiple pathogen ligands, subsequently leading to QDR, each component participating partially to QDR to *Xcc*. This work constitutes a strong basis for deciphering molecular mechanisms involved in the perception systems related to QDR.

Materials and methods

Plant material

Arabidopsis plants were grown on Jiffy pots under controlled conditions (Lacomme and Roby 1996), in a growth chamber at 22 °C with a 9-h photoperiod at 192 µmol m^{-2} s^{-1}. We used the wild-type line Columbia (Col-0) (Wilson et al. 2001; Li et al. 2006) and the following mutant lines (all in Col-0 background): *rks1-1* (Huard-Chauveau et al. 2013), other mutants from the GABI-kat (http://www.gabi-kat.de) or SALK (http://signal.salk.edu) seed libraries and the susceptible accession to *Xcc*568 Kas-1 (Huard-Chauveau et al. 2013). For each mutant line, the T-DNA insertion was determined by sequencing of the T-DNA borders (GABi o8409 or LBb1.3_SALK primer) and of the flanking regions (Supplementary Table S4). The double mutant *mik2-1/rks1-1* was obtained by crossing *mik2-1* pistils with *rks1-1* pollen.

For transient expression assays, *N. benthamiana* plants were cultivated 4-week at 21 °C and under 15 h light period/9 h dark period.

Bacterial material

Agrobacterium tumefaciens strains GV3101, GV3103, and C58C1 were grown at 28 °C on YEB medium with 50 µg.mL^{-1} rifampicin, complemented with 10 µg.mL^{-1} kanamycin and 10 µg.mL^{-1} gentamicin (GV3101), with 100 µg.mL^{-1} carbenicillin and 10 µg.mL^{-1} gentamicin (GV3103) or tetracyclin (C58C1). For transient expression assays for fluorescence microscopy, the Agrobacterium strain GV3101 carrying the corresponding mRFP1 and eGFP constructs was used. Arabidopsis seedlings were transformed according to Marion et al. (2008). Overnight cultures of *A. tumefaciens* were resuspended in 5% sucrose supplemented with acetosyringone (200 µM). Then, 1 week-old seedling were vacuum-infiltrated with the *Agrobacterium* solution. For co-immunoprecipitation

experiments, *Agrobacterium* strain C58C1 carrying the corresponding HA and c-myc constructs was prepared as GV3101 strain. *N. benthamiana* plants were infiltrated and leaf disks harvested 28 h after inoculation.

Xcc inoculation tests were done with the strain LMG568/ATCC33913 (*Xcc568*) (Da Silva et al. 2002). Cultures of *Xcc568* were grown at 28 °C on Kado medium (Kado and Heskett 1970) supplemented with 50 $\mu g.mL^{-1}$ rifampicin and 25 $\mu g.mL^{-1}$ kanamycin.

Constructs and plant transformation

The *MIK2* full length constructs were performed by amplification of the *MIK2* (*AT4G08850*) cDNA coding sequence using, respectively, [attb1_MIK2_full_length and attb4_MIK2_NO_STOP] as primers (Supplementary Table S5). The catalytic $MIK2^{D905A}$ mutants were generated using, respectively, [MIK2_D905A_fw and MIK2_D905A_rev] primers (Supplementary Table S5). MIK2-KinaseDomain was amplified with [attb1_MIK2_KD_fw and attb4_MIK2_NO_STOP] primers (Supplementary Table S5). PCR products were cloned into the multisite Gateway entry vector pBS-DONR P1-P4. 3xHA, 5xc-myc, mRFP1, and eGFP tags were cloned into the entry vector pBS-DONR P4-P2. To fuse *MIK2* constructs with 3xHA, 5xc-myc, mRFP1, or eGFP tags, both vectors were mixed with the 35Sp plant expression vector pEarleyGate100 (Lema Asqui et al. 2018) and recombined with LR clonase II (Invitrogen) described previously (Gu and Innes 2011). We used $RKS1^{D191A}$ in pBS-DONR P1-P4 described in Delplace et al. (2020) fused as MIK2 with c-myc in pEG100. The plasmid constructs with the different tags fused to the genes of interest are reported in the Supplementary Table S6.

The *MIK2-OE/Col-0* and *MIK2-OE/mik2-1* constructs were introduced in the C58C1 *Agrobacterium* strain for transformation of Arabidopsis Col-0 (Clough and Bent 1998). Selection of transformed plants was performed by spraying glufosinate ammonium (BASTA) at 10 $mg.L^{-1}$ on soil-grown plants. Harvested seeds were spread on MS medium containing 50 μM of phosphinothricin for selection of homozygous transgenic plants.

Plant phenotyping and statistical analyses

The disease symptoms of mutant lines were evaluated after inoculation with a bacterial suspension adjusted to 2.10^8 $cfu.mL^{-1}$, in 3 independent experiments (Lacomme and Roby 1996), as compared to Col-0 and *rks1-1*. Four leaves per plant and four 28-day old plants per line were inoculated by piercing and scored as previously described (Meyer et al. 2005), at 0, 3, 5, 7, and 10 days postinoculation.

We fitted the temporal relation of disease index between the tested mutant line and Col-0 by a second order polynomial using the *lm* library under the *R* environment (https://www.R-project.org/). Kinetics of disease index was considered similar if the coefficient of the second order was not significantly different from 0 and if the slope was not significantly different from 1. *P*-value numbers represent kinetic modeling deference with Col-0, $0 = P > 0.05$ and $1 = P \leq 0.05$.

RNA isolation and RT-qPCR

RNA extraction was performed with NucleoSpin RNA plus kit (Macherey-Nagel). RNA extraction was performed with leaves from 28-days-old healthy plants (6 plants and 3 leaves/plant) or inoculated with the *Xcc568* (6 h postinoculation). RT-qPCR analysis was performed as described by Khafif et al. (2017). The gene *AT2G28390* (*MONENSIN SENSITIVITY 1*) was used as an internal control as it is known to be stable in our physiological conditions (Czechowski et al. 2005). Average ΔCp was calculated from three experiments and data were expressed as fold induction for each point as compared to the wild type. Primers have been designed via the Roche website (http://www.lifescience.roche.com) (Supplementary Tables S7 and S8). Results were analyzed using the LC480 on-board software, release version 1.5.0.39. Statistical results were generated with a GLM procedure under the *R* environment. A correction for the number of tests was performed to control the false discovery rate (FDR) at a nominal level of 5%.

Co-immunoprecipitation assays

Total proteins were extracted from *N. benthamiana* leaves harvested 28 h after treatment (transient expression experiments) using the extraction buffer [10% glycerol, 50 mM Tris-HCl pH 8, 150 mM NaCl, 1 mM DTT, 0.05% Nonidet P-40, cOmplete Mini EDTA-Free protease inhibitor cocktail (Sigma), PhosSTOP EASYpack phosphatase inhibitors (Roche) and a spatula tip of polyvinylpolypyrrolidone]. The samples were incubated with anti-c-myc or anti-HA magnetic beads (Thermo Scientific) for 2–4 h and washed with the same buffer without phosphatase inhibitors. Proteins were then separated on SDS-PAGE 4%–15%. After incubation with rat anti-HA:HRP (3F10 clone, Roche [dilution 1:3000]) or mouse anti-Myc:HRP antibodies (9E10 clone, Roche [dilution 1:3000]), proteins were visualized using the Bio-Rad Clarity Western ECL kit and the ChemiDoc Imaging System (Biorad).

Fluorescence microscopy

Fluorescence images were acquired using a Leica SP8 confocal microscope equipped with a water immersion objective lens (25×, numerical aperture 1.20; PL APO) (Imaging TRI-Genotoul plateform). GFP and RFP fluorescence was excited with the 488 nm ray line of the argon laser (10% intensity) or the 552 nm ray line of the He–Ne laser (10% intensity) respectively. The emission recording bands were set in the 505 to 530 nm range for GFP detection, hybrid detector at 100%, and 580 and 620 nm range for RFP detection, with a PMT gain of 775 V. Image acquisition was done in the sequential mode using Leica LCS software and analyzed using the ImageJ software. Representative confocal images are shown after histogram normalization.

Bimolecular fluorescence complementation

The coding sequences of *RSK1*, *MIK2*, and *ZAR1* were amplified by PCR from Arabidopsis Col-0 cDNA using the primers indicated in Supplementary Table S4. To generate C-terminal fusion proteins with the C-terminal or N-terminal fragment of YFP, the genes were cloned into the expression vectors pEG100 (Earley et al. 2006) using the Gateway technology (Invitrogen) (Gu and Innes 2011). The constructs expressing cYFP- or nYFP-tagged proteins in pEG100 were co-transfected into Arabidopsis Col-0 mesophyll protoplasts according to the previously described protocol (Yoo et al. 2007) and co-transfected in *Nicotiana benthamiana* leaves using GV3101 Agrobacterium strain or GV3103 Agrobacterium strain for MtLRRII-cYFP and MtLYK3-cYFP constructions (Lefebvre et al. 2010). The fluorescence was analyzed 16 h (Arabidopsis) or 36 h (*N. benthamiana*) after transfection by confocal laser microscopy (Leica, SP8). YFP was excited with the 514 nm ray line of the argon laser, at 5% of its nominal power. The emission detection range was set between 525 and 575 nm, with a PMT gain of 909.6 V.

Subnetwork reconstruction

Forty-six experimentally identified interactors of MIK2 were recovered from Arabidopsis BioGRID protein interaction datasets Version 4.0.189 (Oughtred et al. 2019) and from the literature

completed with 8 putative interactors from RK network described in Xi et al. (2019). Details of protein–protein interactions are presented in Dataset 1. RK annotation "ligand-perceiving" and "co-receptor" groups were recovered from Xi et al. (2019). Plant processes for each gene were verified with the current literature. Protein–protein interactions were plotted with Cytoscape software V3.7.2.

Accession numbers

Sequence data referenced in this study are available via the SRA database under accession number SRP233656.

Acknowledgments

We thank Mehdi Khafif for technical assistance in Arabidopsis transient expression assays, Cécile Pouzet for cell imaging and Ullrich Dubiella and Marie Invernizzi for experimental assistance with plasmid constructs and diverse protein interaction tests.

Author contributions

D.R. designed research. F.D. and C.H.-C. performed research. F.D., C.H.-C., F.R., and D.R. analyzed data. F.D., C.H.-C., F.R., and D.R. wrote the paper.

Supplementary data

The following materials are available in the online version of this article.

Supplementary Figure S1. Full-length MIK2 interacts with RKS1.

Supplementary Figure S2. MIK2 physically interacts with RKS1 at the plasma membrane by BiFC in Arabidopsis protoplasts.

Supplementary Figure S3. MIK2 physically interacts with RKS1 at the plasma membrane by BiFC in *N. benthamiana* leaves.

Supplementary Figure S4. *MIK2* expression in mutants and other lines used in this study.

Supplementary Figure S5. *mik2* mutants are more susceptible to *Xcc568* infection.

Supplementary Figure S6. Analysis of *rks1-1*, *mik2-1* and *rks1-1/mik2-1* mutant lines in response to *Xcc568*.

Supplementary Figure S7. Cell wall-sensing mutants are not affected in their QDR to *Xcc568*.

Supplementary Figure S8. Nine endogenous *PROSCOOPs*, including *PROSCOOP12*, are differentially expressed during *Xcc568* infection, similar to the expression pattern of *MIK2*.

Supplementary Figure S9. A SCOOP12-like peptide found in the XopAM effector.

Supplementary Table S1. Gene expression quantified by RT-qPCR six hours after infiltration with *Xcc568* at 2.10^8 cfu/mL.

Supplementary Table S2. Molecular analysis of insertional mutants of the RK network.

Supplementary Table S3. Molecular analysis of insertional mutants of the RKS1-dependent subnetwork.

Supplementary Table S4. List of primers used for mutant genotyping.

Supplementary Table S5. Primers used for *MIK2* constructs.

Supplementary Table S6. List of pEarleyGate100-based constructs used in this study.

Supplementary Table S7. List of RT-qPCR primers used for expression analysis.

Supplementary Table S8. List of RT-qPCR primers used for the molecular characterization of T-DNA mutants.

Supplementary Data Set 1. Protein-protein interactions used to generate the RKS1/MIK2 PPI network.

Funding

This work was supported by the French Agence Nationale de la Recherche (ANR) grant (RIPOSTE ANR-14-OE19-0024-01) and the French Laboratory of Excellence Project TULIP (ANR-10-LABX-41). F.D. is funded by a grant from Région Occitanie and the Plant Health and Environment Division of INRAE.

Conflict of interest statement. None declared.

Data availability

The data underlying this article are available in the article and in its online supplementary material.

References

Adachi H, Kamoun S, Maqbool A. A resistosome-activated 'death switch'. *Nat Plants*. 2019:5(5):457–458. https://doi.org/10.1038/s41477-019-0425-9

Adachi H, Tsuda K. Convergence of cell-surface and intracellular immune receptor signalling. *New Phytol*. 2019:221(4):1676–1678. https://doi.org/10.1111/nph.15634

Ahmed H, Howton TC, Sun Y, Weinberger N, Belkhadir Y, Mukhtar MS. Network biology discovers pathogen contact points in host protein-protein interactomes. *Nat Commun*. 2018:9(1):2312. https://doi.org/10.1038/s41467-018-04632-8

An SQ, Potnis N, Dow M, Vorhölter FJ, He YQ, Becker A, Teper D, Li Y, Wang N, Bleris L, *et al*. Mechanistic insights into host adaptation, virulence and epidemiology of the phytopathogen Xanthomonas. *FEMS Microbiol Rev*. 2020:44(1):1–32. https://doi.org/10.1093/femsre/fuz024

Antolín-Llovera M, Ried MK, Binder A, Parniske M. Receptor kinase signaling pathways in plant-microbe interactions. *Annu Rev Phytopathol*. 2012:50(1):451–473. https://doi.org/10.1146/annurev-phyto-081211-173002

Bani M, Pérez-De-Luque A, Rubiales D, Rispail N. Physical and chemical barriers in root tissues contribute to quantitative resistance to *Fusarium oxysporum* f. sp. pisi in Pea. *Front Plant Sci*. 2018:9:199. https://doi.org/10.3389/fpls.2018.00199

Bauer Z, Gómez-Gómez L, Boller T, Felix G. Sensitivity of different ecotypes and mutants of *Arabidopsis thaliana* toward the bacterial elicitor flagellin correlates with the presence of receptor-binding sites. *J Biol Chem*. 2001:276(49):45669–45676. https://doi.org/10.1074/jbc.M102390200

Blaum BS, Mazzotta S, Nöldeke ER, Halter T, Madlung J, Kemmerling B, Stehle T. Structure of the pseudokinase domain of BIR2, a regulator of BAK1-mediated immune signaling in Arabidopsis. *J Struct Biol*. 2014:186(1):112–121. https://doi.org/10.1016/j.jsb.2014.02.005

Boudeau J, Miranda-Saavedra D, Barton GJ, Alessi DR. Emerging roles of pseudokinases. *Trends Cell Biol*. 2006:16(9):443–452. https://doi.org/10.1016/j.tcb.2006.07.003

Broglie KE, Butler KH, Butruille MG, da Silva Conceição A, Frey TJ, Hawk JA, Jaqueth JS, Jones ES, Multani DS, Wolters PJ. Method for identifying maize plants with RCG1 gene conferring resistance to colletotrichum infection. Patent US8062847B2. 2006.

Burkart RC, Stahl Y. Dynamic complexity: plant receptor complexes at the plasma membrane. *Curr Opin Plant Biol*. 2017:40:15–21. https://doi.org/10.1016/j.pbi.2017.06.016

Chan C, Panzeri D, Okuma E, Tõldsepp K, Wang YY, Louh GY, Chin TC, Yeh YH, Yeh HL, Yekondi S, *et al.* Stress induced factor 2 regulates arabidopsis stomatal immunity through phosphorylation of the anion channel SLAC1. *Plant Cell*. 2020:32(7):2216–2236. https://doi.org/10.1105/tpc.19.00578

Cheung AY, Wu HM. THESEUS 1, FERONIA and relatives: a family of cell wall-sensing receptor kinases? *Curr Opin Plant Biol*. 2011:14(6):632–641. https://doi.org/10.1016/j.pbi.2011.09.001

Chinchilla D, Bauer Z, Regenass M, Boller T, Felix G. The Arabidopsis receptor kinase FLS2 binds flg22 and determines the specificity of flagellin perception. *Plant Cell*. 2006:18(2):465–476. https://doi.org/10.1105/tpc.105.036574

Clough SJ, Bent AF. Floral dip: a simplified method for Agrobacterium-mediated transformation of *Arabidopsis thaliana*. *Plant J*. 1998:16(6):735–743. https://doi.org/10.1046/j.1365-313x.1998.00343.x

Coleman AD, Maroschek J, Raasch L, Takken FLW, Ranf S, Hückelhoven R. The Arabidopsis leucine-rich repeat receptor-like kinase MIK2 is a crucial component of early immune responses to a fungal-derived elicitor. *New Phytol*. 2020:229(6):3453–3466. https://doi.org/10.1111/nph.17122

Contreras MP, Lüdke D, Pai H, Toghani A, Kamoun S. NLR receptors in plant immunity: making sense of the alphabet soup. *EMBO Rep*. 2023:24(10):e57495. https://doi.org/10.15252/embr.202357495

Cook DE, Mesarich CH, Thomma BP. Understanding plant immunity as a surveillance system to detect invasion. *Annu Rev Phytopathol*. 2015:53(1):541–563. https://doi.org/10.1146/annurev-phyto-080614-120114

Corwin JA, Kliebenstein DJ. Quantitative resistance: more than just perception of a pathogen. *Plant Cell*. 2017:29(4):655–665. https://doi.org/10.1105/tpc.16.00915

Crook AD, Willoughby AC, Hazak O, Okuda S, VanDerMolen KR, Soyars CL, Cattaneo P, Clark NM, Sozzani R, Hothorn M, *et al.* BAM1/2 receptor kinase signaling drives CLE peptide-mediated formative cell divisions in Arabidopsis roots. *Proc Natl Acad Sci U S A*. 2020:117(51):32750–32756. https://doi.org/10.1073/pnas.2018565117

Cui Y, Hu C, Zhu Y, Cheng K, Li X, Wei Z, Xue L, Lin F, Shi H, Yi J, *et al.* Cik receptor kinases determine cell fate specificatioduring early anther development in Arabidopsis. *Plant Cell*. 2018:30(10):2383–2401. https://doi.org/10.1105/tpc.17.00586

Czechowski T, Stitt M, Altmann T, Udvardi MK, Scheible WR. Genome-wide identification and testing of superior reference genes for transcript normalization in Arabidopsis. *Plant Physiol*. 2005:139(1):5–17. https://doi.org/10.1104/pp.105.063743

da Silva AC, Ferro JA, Reinach FC, Farah CS, Furlan LR, Quaggio RB, Monteiro-Vitorello CB, Van Sluys MA, Almeida NF, Alves LM, *et al.* Comparison of the genomes of two Xanthomonas pathogens with differing host specificities. *Nature*. 2002:417(6887):459–463. https://doi.org/10.1038/417459a

Degrave A, Siamer S, Boureau T, Barny MA. The AvrE superfamily: ancestral type III effectors involved in suppression of pathogen-associated molecular pattern-triggered immunity. *Mol Plant Pathol*. 2015:16(8):899–905. https://doi.org/10.1111/mpp.12237

Delplace F, Huard-Chauveau C, Berthomé R, Roby D. Network organization of the plant immune system: from pathogen perception to robust defense induction. *Plant J*. 2022:109(2):447–470. https://doi.org/10.1111/tpj.15462

Delplace F, Huard-Chauveau C, Dubiella U, Khafif M, Alvarez E, Langin G, Roux F, Peyraud R, Roby D. Robustness of plant quantitative disease resistance is provided by a decentralized immune network. *Proc Natl Acad Sci U S A*. 2020:117(30):18099–18109. https://doi.org/10.1073/pnas.2000078117

Demirjian C, Razavi N, Yu G, Mayjonade B, Zhang L, Lonjon F, Chardon F, Carrere S, Gouzy J, Genin S, *et al.* An atypical NLR gene confers bacterial wilt susceptibility in Arabidopsis. *Plant Commun*. 2023a:4(5):100607. https://doi.org/10.1016/j.xplc.2023.100607

Demirjian C, Vailleau F, Berthomé R, Roux F. Genome-wide association studies in plant pathosystems: success or failure? *Trends Plant Sci*. 2023b:28(4):471–485. https://doi.org/10.1016/j.tplants.2022.11.006

Duckney P, Deeks MJ, Dixon MR, Kroon J, Hawkins TJ, Hussey PJ. Actin-membrane interactions mediated by NETWORKED2 in Arabidopsis pollen tubes through associations with pollen receptor-like kinase 4 and 5. *New Phytol*. 2017:216(4):1170–1180. https://doi.org/10.1111/nph.14745

Earley KW, Haag JR, Pontes O, Opper K, Juehne T, Song K, Pikaard CS. Gateway-compatible vectors for plant functional genomics and proteomics. First published: 26 January 2006. https://doi.org/10.1111/j.1365-313X.2005.02617.x

French E, Kim BS, Iyer-Pascuzzi AS. Mechanisms of quantitative disease resistance in plants. *Semin Cell Dev Biol*. 2016:56:201–208. https://doi.org/10.1016/j.semcdb.2016.05.015

Froidure S, Canonne J, Daniel X, Jauneau A, Brière C, Roby D, Rivas S. AtsPLA2-α nuclear relocalization by the Arabidopsis transcription factor AtMYB30 leads to repression of the plant defense response. *Proc Natl Acad Sci U S A*. 2010:107(34):15281–15286. https://doi.org/10.1073/pnas.1009056107

Fukuoka S, Yamamoto SI, Mizobuchi R, Yamanouchi U, Ono K, Kitazawa N, Yasuda N, Fujita Y, Thi Thanh Nguyen T, Koizumi S, *et al.* Multiple functional polymorphisms in a single disease resistance gene in rice enhance durable resistance to blast. *Sci Rep*. 2014:4(1):4550. https://doi.org/10.1038/srep04550

Glazebrook J. Contrasting mechanisms of defense against biotrophic and necrotrophic pathogens. *Annu Rev Phytopathol*. 2005:43(1):205–227. https://doi.org/10.1146/annurev.phyto.43.040204.135923

Gómez-Gómez L, Boller T. FLS2: an LRR receptor-like kinase involved in the perception of the bacterial elicitor flagellin in Arabidopsis. *Mol Cell*. 2000:5(6):1003–1011. https://doi.org/10.1016/S1097-2765(00)80265-8

Gu Y, Innes RW. The KEEP on going protein of Arabidopsis recruits the ENHANCED DISEASE RESISTANCE1 protein to trans-Golgi network/early endosome vesicles. *Plant Physiol*. 2011:155(4):1827–1838. https://doi.org/10.1104/pp.110.171785

Guy E, Genissel A, Hajri A, Chabannes M, David P, Carrere S, Lautier M, Roux B, Boureau T, Arlat M, *et al.* Natural genetic variation of *Xanthomonas campestris* pv. *campestris* pathogenicity on Arabidopsis revealed by association and reverse genetics. *mBio*. 2013:4(3):e00538. https://doi.org/10.1128/mBio.00538-12

Halter T, Imkampe J, Blaum BS, Stehle T, Kemmerling B. BIR2 affects complex formation of BAK1 with ligand binding receptors in plant defense. *Plant Signal Behav*. 2014a:9(6):e28944. https://doi.org/10.4161/psb.28944

Halter T, Imkampe J, Mazzotta S, Wierzba M, Postel S, Bücherl C, Kiefer C, Stahl M, Chinchilla D, Wang X, *et al.* The leucine-rich repeat receptor kinase BIR2 is a negative regulator of BAK1 in plant immunity. *Curr Biol*. 2014b:24(2):134–143. https://doi.org/10.1016/j.cub.2013.11.047

He Y, Gao J, Luo M, Gao C, Lin Y, Wong HY, Cui Y, Zhuang X, Jiang L. VAMP724 and VAMP726 are involved in autophagosome formation in *Arabidopsis thaliana*. *Autophagy*. 2023:19(5):1406–1423. https://doi.org/10.1080/15548627.2022.2127240

He Y, Zhou J, Shan L, Meng X. Plant cell surface receptor-mediated signaling—a common theme amid diversity. *J Cell Sci*. 2018:131(2):jcs209353. https://doi.org/10.1242/jcs.209353

Holton N, Nekrasov V, Ronald PC, Zipfel C. The phylogenetically-related pattern recognition receptors EFR and XA21 recruit similar immune signaling components in monocots and dicots. *PLoS Pathog*. 2015:11(1):e1004602. https://doi.org/10.1371/journal.ppat.1004602

Hou S, Liu D, Huang S, Luo D, Liu Z, Xiang Q, Wang P, Mu R, Han Z, Chen S, *et al*. The Arabidopsis MIK2 receptor elicits immunity by sensing a conserved signature from phytocytokines and microbes. *Nat Commun*. 2021:12(1):5494. https://doi.org/10.1038/s41467-021-25580-w

Huard-Chauveau C, Perchepied L, Debieu M, Rivas S, Kroj T, Kars I, Bergelson J, Roux F, Roby D. An atypical kinase under balancing selection confers broad-spectrum disease resistance in Arabidopsis. *PLoS Genet*. 2013:9(9):e1003766. https://doi.org/10.1371/journal.pgen.1003766

Julkowska MM, Klei K, Fokkens L, Haring MA, Schranz ME, Testerink C. Natural variation in rosette size under salt stress conditions corresponds to developmental differences between Arabidopsis accessions and allelic variation in the LRR-KISS gene. *J Exp Bot*. 2016:67(8):2127–2138. https://doi.org/10.1093/jxb/erw015

Kado CI, Heskett MG. Selective media for isolation of agrobacterium, corynebacterium, erwinia, pseudomonas, and xanthomonas. *Phytopathology*. 1970:60(6):969–976. https://doi.org/10.1094/Phyto-60-969

Kanyuka K, Rudd JJ. Cell surface immune receptors: the guardians of the plant's extracellular spaces. *Curr Opin Plant Biol*. 2019:50:1–8. https://doi.org/10.1016/j.pbi.2019.02.005

Kemmerling B, Schwedt A, Rodriguez P, Mazzotta S, Frank M, Qamar SA, Mengiste T, Betsuyaku S, Parker JE, Müssig C, *et al*. The BRI1-associated kinase 1, BAK1, has a brassinolide-independent role in plant cell-death control. *Curr Biol*. 2007:17(13):1116–1122. https://doi.org/10.1016/j.cub.2007.05.046

Khafif M, Balagué C, Huard-Chauveau C, Roby D. An essential role for the VASt domain of the Arabidopsis VAD1 protein in the regulation of defense and cell death in response to pathogens. *PLoS One*. 2017:12(7):e0179782. https://doi.org/10.1371/journal.pone.0179782

Kubicek CP, Starr TL, Glass NL. Plant cell wall–degrading enzymes and their secretion in plant-pathogenic fungi. *Annu Rev Phytopathol*. 2014:52(1):427–451. https://doi.org/10.1146/annurev-phyto-102313-045831

Kunze G, Zipfel C, Robatzek S, Niehaus K, Boller T, Felix G. The N terminus of bacterial elongation factor Tu elicits innate immunity in Arabidopsis plants. *Plant Cell*. 2004:16(12):3496–3507. https://doi.org/10.1105/tpc.104.026765

Lacomme C, Roby D. Molecular cloning of a sulfotransferase in *Arabidopsis thaliana* and regulation during development and in response to infection with pathogenic bacteria. *Plant Mol Biol*. 1996:30(5):995–1008. https://doi.org/10.1007/BF00020810

Laohavisit A, Wakatake T, Ishihama N, Mulvey H, Takizawa K, Suzuki T, Shirasu K. Quinone perception in plants via leucine-rich-repeat receptor-like kinases. *Nature*. 2020:587(7832):92–97. https://doi.org/10.1038/s41586-020-2655-4

Lefebvre B, Timmers T, Mbengue M, Moreau S, Hervé C, Tóth K, Bittencourt-Silvestre J, Klaus D, Deslandes L, Godiard L, *et al*. A remorin protein interacts with symbiotic receptors and regulates bacterial infection. *Proc Natl Acad Sci U S A*. 2010:107(5):2343–2348. https://doi.org/10.1073/pnas.0913320107

Lema Asqui S, Vercammen D, Serrano I, Valls M, Rivas S, Van Breusegem F, Conlon FL, Dangl JL, Coll NS. AtSERPIN1 is an inhibitor of the metacaspase AtMC1-mediated cell death and autocatalytic processing in planta. *New Phytol*. 2018:218(3):1156–1166. https://doi.org/10.1111/nph.14446

Li Y, Roycewicz P, Smith E, Borevitz JO. Genetics of local adaptation in the laboratory: flowering time quantitative trait loci under geographic and seasonal conditions in Arabidopsis. *PLoS One*. 2006:1(1):e105. https://doi.org/10.1371/journal.pone.0000105

Lin W, Ma X, Shan L, He P. Big roles of small kinases: the complex functions of receptor-like cytoplasmic kinases in plant immunity and development. *J Integr Plant Biol*. 2013:55(12):1188–1197. https://doi.org/10.1111/jipb.12071

Liu F, Zeng M, Sun Y, Chen Z, Chen Z, Wang L, Cui JR, Zhang F, Lv D, Chen X, *et al*. BAK1 protects the receptor-like kinase BIR2 from SNIPER2a/b-mediated degradation to promote pattern-triggered immunity in *Nicotiana benthamiana*. *Plant Cell*. 2023:35(9):3566–3584. https://doi.org/10.1093/plcell/koad187

Liu Y, Huang X, Li M, He P, Zhang Y. Loss-of-function of Arabidopsis receptor-like kinase BIR1 activates cell death and defense responses mediated by BAK1 and SOBIR1. *New Phytol*. 2016:212(3):637–645. https://doi.org/10.1111/nph.14072

Marion J, Bach L, Bellec Y, Meyer C, Gissot L, Faure JD. Systematic analysis of protein subcellular localization and interaction using high-throughput transient transformation of Arabidopsis seedlings. *Plant J*. 2008:56(1):169–179. https://doi.org/10.1111/j.1365-313X.2008.03596.x

Mata-Pérez C, Sánchez-Calvo B, Begara-Morales JC, Luque F, Jiménez-Ruiz J, Padilla MN, Fierro-Risco J, Valderrama R, Fernández-Ocaña A, Corpas FJ, *et al*. Transcriptomic profiling of linolenic acid-responsive genes in ROS signaling from RNA-seq data in Arabidopsis. *Front Plant Sci*. 2015:6:122. https://doi.org/10.3389/fpls.2015.00122

Mendy B, Wang'ombe MW, Radakovic ZS, Holbein J, Ilyas M, Chopra D, Holton N, Zipfel C, Grundler FM, Siddique S. Arabidopsis leucine-rich repeat receptor–like kinase NILR1 is required for induction of innate immunity to parasitic nematodes. *PLoS Pathog*. 2017:13(4):e1006284. https://doi.org/10.1371/journal.ppat.1006284

Meyer D, Lauber E, Roby D, Arlat M, Kroj T. Optimization of pathogenicity assays to study the *Arabidopsis thaliana-Xanthomonas campestris* pv. *campestris* pathosystem. *Mol Plant Pathol*. 2005:6(3):327–333. https://doi.org/10.1111/j.1364-3703.2005.00287.x

Monaghan J, Zipfel C. Plant pattern recognition receptor complexes at the plasma membrane. *Curr Opin Plant Biol*. 2012:15(4):349–357. https://doi.org/10.1016/j.pbi.2012.05.006

Murphy JM, Mace PD, Eyers PA. Live and let die: insights into pseudoenzyme mechanisms from structure. *Curr Opin Struct Biol*. 2017:47:95–104. https://doi.org/10.1016/j.sbi.2017.07.004

Nelson R, Wiesner-Hanks T, Wisser R, Balint-Kurti P. Navigating complexity to breed disease-resistant crops. *Nat Rev Genet*. 2018:19(1):21–33. https://doi.org/10.1038/nrg.2017.82

Ngou BPM, Ahn HK, Ding P, Jones JDG. Mutual potentiation of plant immunity by cell-surface and intracellular receptors. *Nature*. 2021:592(7852):110–115. https://doi.org/10.1038/s41586-021-03315-7

Ngou BPM, Ding P, Jones JDG. Thirty years of resistance: Zig-zag through the plant immune system. *Plant Cell*. 2022:34(5):1447–1478. https://doi.org/10.1093/plcell/koac041

Nissen KS, Willats WGT, Malinovsky FG. Understanding CrRLK1L function: cell walls and growth control. *Trends Plant Sci*. 2016:21(6):516–527. https://doi.org/10.1016/j.tplants.2015.12.004

Oh MH, Wang X, Clouse SD, Huber SC. Deactivation of the Arabidopsis brassinosteroid insensitive 1 (BRI1) receptor kinase by autophosphorylation within the glycine-rich loop. *Proc Natl Acad Sci U S A*. 2012:109(1):327–332. https://doi.org/10.1073/pnas.1108321109

Oh MH, Wang X, Wu X, Zhao Y, Clouse SD, Huber SC. Autophosphorylation of Tyr-610 in the receptor kinase BAK1 plays a role in brassinosteroid signaling and basal defense gene

expression. *Proc Natl Acad Sci U S A*. 2010:107(41):17827–17832. https://doi.org/10.1073/pnas.0915064107

Oughtred R, Stark C, Breitkreutz BJ, Rust J, Boucher L, Chang C, Kolas N, O'Donnell L, Leung G, McAdam R, *et al.* The BioGRID interaction database: 2019 update. *Nucleic Acids Res*. 2019:47(D1): D529–D541. https://doi.org/10.1093/nar/gky1079

Panstruga R, Parker JE, Schulze-Lefert P. SnapShot: plant immune response pathways. *Cell*. 2009:136(5):978.e1–978.e3. https://doi.org/10.1016/j.cell.2009.02.020

Pilet-Nayel ML, Moury B, Caffier V, Montarry J, Kerlan MC, Fournet S, Durel CE, Delourme R. Quantitative resistance to plant pathogens in pyramiding strategies for durable crop protection. *Front Plant Sci*. 2017:8:1838. https://doi.org/10.3389/fpls.2017.01838

Poland JA, Balint-Kurti PJ, Wisser RJ, Pratt RC, Nelson RJ. Shades of gray: the world of quantitative disease resistance. *Trends Plant Sci*. 2009:14(1):21–29. https://doi.org/10.1016/j.tplants.2008.10.006

Postel S, Küfner I, Beuter C, Mazzotta S, Schwedt A, Borlotti A, Halter T, Kemmerling B, Nürnberger T. The multifunctional leucine-rich repeat receptor kinase BAK1 is implicated in Arabidopsis development and immunity. *Eur J Cell Biol*. 2010:89(2-3):169–174. https://doi.org/10.1016/j.ejcb.2009.11.001

Potnis N, Krasileva K, Chow V, Almeida NF, Patil PB, Ryan RP, Sharlach M, Behlau F, Dow JM, Momol M, *et al.* Comparative genomics reveals diversity among xanthomonads infecting tomato and pepper. *BMC Genomics*. 2011:12(1):146. https://doi.org/10.1186/1471-2164-12-146

Reiterer V, Eyers PA, Farhan H. Day of the dead: pseudokinases and pseudophosphatases in physiology and disease. *Trends Cell Biol*. 2014:24(9):489–505. https://doi.org/10.1016/j.tcb.2014.03.008

Ren H, Willige BC, Jaillais Y, Geng S, Park MY, Gray WM, Chory J. BRASSINOSTEROID-SIGNALING KINASE 3, a plasma membrane-associated scaffold protein involved in early brassinosteroid signaling. *PLoS Genet*. 2019:15(1):e1007904. https://doi.org/10.1371/journal.pgen.1007904

Rhodes J, Yang H, Moussu S, Boutrot F, Santiago J, Zipfel C. Perception of a divergent family of phytocytokines by the Arabidopsis receptor kinase MIK2. *Nat Commun*. 2021:12(1):705. https://doi.org/10.1038/s41467-021-20932-y

Roux F, Noël L, Rivas S, Roby D. ZRK atypical kinases: emerging signaling components of plant immunity. *New Phytol*. 2014a:203(3): 713–716. https://doi.org/10.1111/nph.12841

Roux F, Voisin D, Badet T, Balagué C, Barlet X, Huard-Chauveau C, Roby D, Raffaele S. Resistance to phytopathogens e tutti quanti : placing plant quantitative disease resistance on the map. *Mol Plant Pathol*. 2014b:15(5):427–432. https://doi.org/10.1111/mpp.12138

Wang J, Wang J, Hu M, Wu S, Qi J, Wang G, Han Z, Qi Y, Gao N, Wang H-W, *et al.* Ligand-triggered allosteric ADP release primes a plant NLR complex. *Science*. 2019:364:eaav5868. https://doi.org/10.1126/science.aav5868

Scarpeci TE, Zanor MI, Mueller-Roeber B, Valle EM. Overexpression of AtWRKY30 enhances abiotic stress tolerance during early growth stages in Arabidopsis thaliana. *Plant Mol Biol*. 2013:83: 265-277. https://doi.org/10.1007/s11103-013-0090-8

Smakowska-Luzan E, Mott GA, Parys K, Stegmann M, Howton TC, Layeghifard M, Neuhold J, Lehner A, Kong J, Grünwald K, *et al.* An extracellular network of Arabidopsis leucine-rich repeat receptor kinases. *Nature*. 2018:553(7688):342–346. https://doi.org/10.1038/nature25184

Sreeramulu S, Mostizky Y, Sunitha S, Shani E, Nahum H, Salomon D, Hayun LB, Gruetter C, Rauh D, Ori N, *et al.* BSKs are partially redundant positive regulators of brassinosteroid signaling in Arabidopsis. *Plant J*. 2013:74(6):905–919. https://doi.org/10.1111/tpj.12175

Staal J, Kaliff M, Bohman S, Dixelius C. Transgressive segregation reveals two Arabidopsis TIR-NB-LRR resistance genes effective against *Leptosphaeria maculans*, causal agent of blackleg disease. *Plant J*. 2006:46(2):218–230. https://doi.org/10.1111/j.1365-313X.2006.02688.x

Stegmann M, Monaghan J, Smakowska-Luzan E, Rovenich H, Lehner A, Holton N, Belkhadir Y, Zipfel C. The receptor kinase FER is a RALF-regulated scaffold controlling plant immune signaling. *Science*. 2017:355(6322):287–289. https://doi.org/10.1126/science.aal2541

Suzuki M, Watanabe T, Yoshida I, Kaku H, Shibuya N. Autophosphorylation site Y428 is essential for the in vivo activation of CERK1. *Plant Signal Behav*. 2018:13(2):e1435228. https://doi.org/10.1080/15592324.2018.1435228

Takeuchi H, Higashiyama T. Tip-localized receptors control pollen tube growth and LURE sensing in Arabidopsis. *Nature*. 2016:531: 245-248. https://doi.org/10.1038/nature17413

Tang D, Wang G, Zhou JM. Receptor kinases in plant-pathogen interactions: more than pattern recognition. *Plant Cell*. 2017:29(4): 618–637. https://doi.org/10.1105/tpc.16.00891

van der Burgh AM, Postma J, Robatzek S, Joosten MHAJ. Kinase activity of SOBIR1 and BAK1 is required for immune signalling. *Mol Plant Pathol*. 2019:20(3):410–422. https://doi.org/10.1111/mpp.12767

Van der Does D, Boutrot F, Engelsdorf T, Rhodes J, McKenna JF, Vernhettes S, Koevoets I, Tintor N, Veerabagu M, Miedes E, *et al.* The Arabidopsis leucine-rich repeat receptor kinase MIK2/LRR-KISS connects cell wall integrity sensing, root growth and response to abiotic and biotic stresses. *PLoS Genet*. 2017:13(6): e1006832. https://doi.org/10.1371/journal.pgen.1006832

Wang G, Roux B, Feng F, Guy E, Li L, Li N, Zhang X, Lautier M, Jardinaud MF, Chabannes M, *et al.* The decoy substrate of a pathogen effector and a pseudokinase specify pathogen-induced modified-self recognition and immunity in plants. *Cell Host Microbe*. 2015:18(3):285–295. https://doi.org/10.1016/j.chom.2015.08.004

Wang T, Liang L, Xue Y, Jia PF, Chen W, Zhang MX, Wang YC, Li HJ, Yang WC. A receptor heteromer mediates the male perception of female attractants in plants. *Nature*. 2016:531(7593):241–244. https://doi.org/10.1038/nature16975

Wang J, Wang J, Hu M, Wu S, Qi J, Wang G, Han Z, Qi Y, Gao N, Wang H-W, *et al.* Ligand-triggered allosteric ADP release primes a plant NLR complex. *Science*. 2019:364:eaav5868. https://doi.org/10.1126/science.aav5868

Wilson IW, Schiff CL, Hughes DE, Somerville SC. Quantitative trait loci analysis of powdery mildew disease resistance in the *Arabidopsis thaliana* accession Kashmir-1. *Genetics*. 2001:158(3): 1301–1309. https://doi.org/10.1093/genetics/158.3.1301

Wróblewski T, Spiridon L, Martin EC, Petrescu AJ, Cavanaugh K, Truco MJ, Xu H, Gozdowski D, Pawłowski K, Michelmore RW, *et al.* Genome-wide functional analyses of plant coiled–coil NLR-type pathogen receptors reveal essential roles of their N-terminal domain in oligomerization, networking, and immunity. *PLoS Biol*. 2018:16(12):e2005821. https://doi.org/10.1371/journal.pbio.2005821

Wu CH, Derevnina L, Kamoun S. Receptor networks underpin plant immunity. *Science*. 2018:360(6395):1300–1301. https://doi.org/10.1126/science.aat2623

Xi L, Wu XN, Gilbert M, Schulze WX. Classification and interactions of LRR receptors and co-receptors within the Arabidopsis plasma membrane—an overview. *Front Plant Sci*. 2019:10:472. https://doi.org/10.3389/fpls.2019.00472

Xie Q, Wei B, Zhan Z, He Q, Wu K, Chen Y, Liu S, He C, Niu X, Li C, *et al*. Arabidopsis membrane protein AMAR1 interaction with type III effector XopAM triggers a hypersensitive response. *Plant Physiol*. 2023:193(4):2768–2787. https://doi.org/10.1093/plphys/kiad478

Yang H, Kim X, Skłenar J, Aubourg S, Sancho-Andrés G, Stahl E, Guillou MC, Gigli-Bisceglia N, Tran Van Canh L, Bender KW, *et al*. Subtilase-mediated biogenesis of the expanded family of SERINE RICH ENDOGENOUS PEPTIDES. *Nat Plants*. 2023:9(12): 2085–2094. https://doi.org/10.1038/s41477-023-01583-x

Yeh YH, Panzeri D, Kadota Y, Huang YC, Huang PY, Tao CN, Roux M, Chien HC, Chin TC, Chu PW, *et al*. The Arabidopsis malectin-like/LRR-RLK IOS1 is critical for BAK1-dependent and BAK1-independent pattern-triggered immunity. *Plant Cell*. 2016:28(7): 1701–1721. https://doi.org/10.1105/tpc.16.00313

Yoo SD, Cho YH, Sheen J. Arabidopsis mesophyll protoplasts: a versatile cell system for transient gene expression analysis. *Nat Protocols*. 2007:2(7):1565–1572. https://doi.org/10.1038/nprot.2007.199

Yu J, Kang L, Li Y, Wu C, Zheng C, Liu P, Huang J. RING finger protein RGLG1 and RGLG2 negatively modulate MAPKKK18 mediated drought stress tolerance in Arabidopsis. *J Integr Plant Biol*. 2020:63(3):484–493. https://doi.org/10.1111/jipb.13019

Zhang X, Peng H, Zhu S, Xing J, Li X, Zhu Z, Zheng J, Wang L, Wang B, Chen J, *et al*. Nematode–encoded RALF peptide mimics facilitate parasitism of plants through the FERONIA receptor kinase. *Mol Plant*. 2020:13(10):1434–1454.

Zhou J, Wang P, Claus LAN, Savatin DV, Xu G, Wu S, Meng X, Russinova E, He P, Shan L. Proteolytic processing of serk3/bak1 regulates plant immunity, development, and cell death. *Plant Physiol*. 2019:180(1):543–558. https://doi.org/10.1104/pp.18.01503

Zipfel C, Kunze G, Chinchilla D, Caniard A, Jones JD, Boller T, Felix G. Perception of the bacterial PAMP EF-Tu by the receptor EFR restricts agrobacterium-mediated transformation. *Cell*. 2006: 125(4):749–760. https://doi.org/10.1016/j.cell.2006.03.037

Zuo W, Chao Q, Zhang N, Ye J, Tan G, Li B, Xing Y, Zhang B, Liu H, Fengler KA, *et al*. A maize wall-associated kinase confers quantitative resistance to head smut. *Nat Genet*. 2015:47(2):151–157. https://doi.org/10.1038/ng.3170